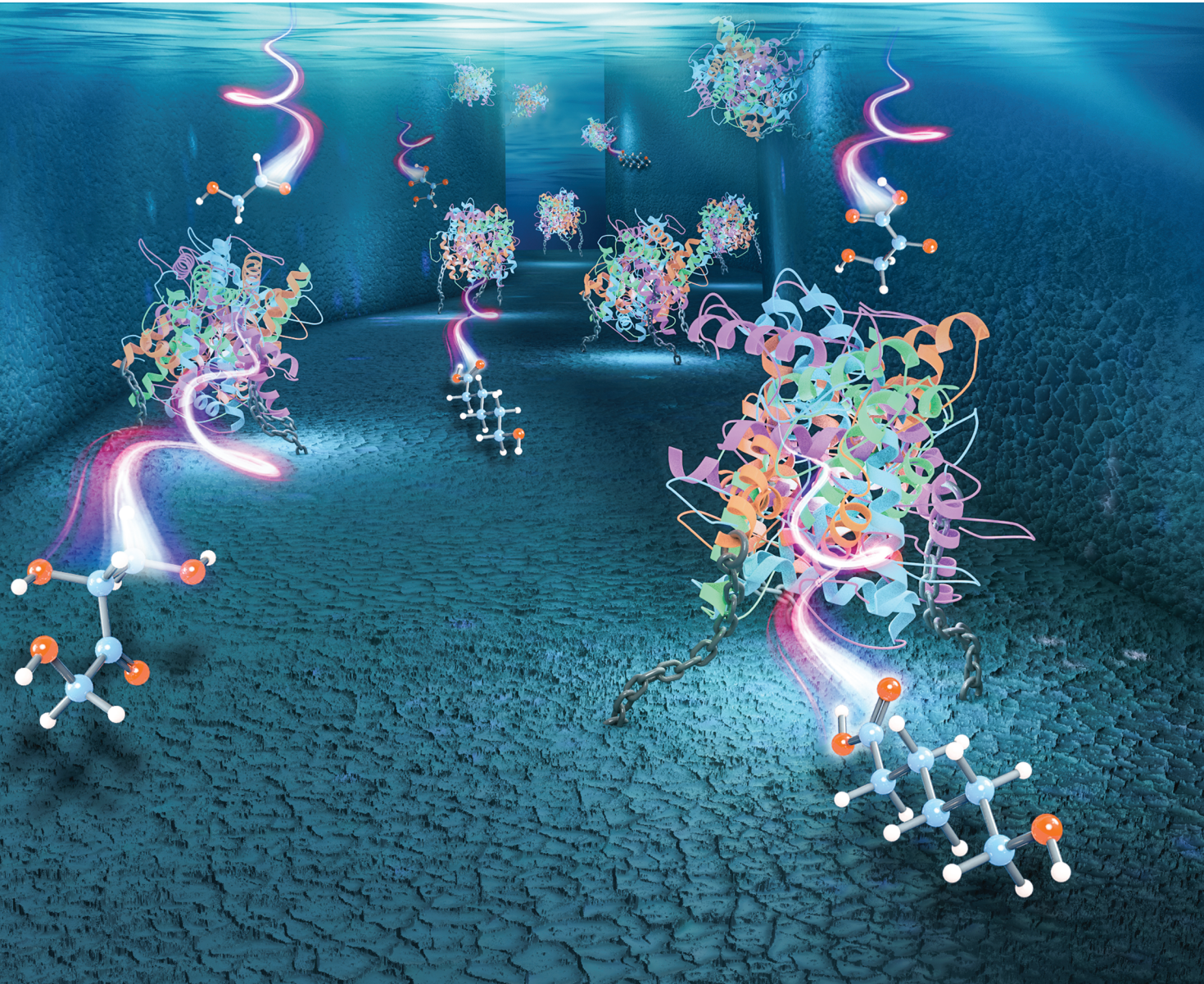


Reaction Chemistry & Engineering

Linking fundamental chemistry and engineering to create scalable, efficient processes

rsc.li/reaction-engineering



ISSN 2058-9883

REVIEW



Cite this: *React. Chem. Eng.*, 2020,
5, 9

Microfluidic immobilized enzyme reactors for continuous biocatalysis

Yujiao Zhu, abc Qingming Chen, ab Liyang Shao, d Yanwei Jia^cef and Xuming Zhang *ab

Biocatalysis has attracted significant attention owing to its environmental-friendly nature, high efficiency, and remarkable selectivity for reactions. However, enzymes, which are powerful catalysts used in biocatalysis, suffer from low stability when used for long-term operations in solution and a gradual decrease in activity during storage. Microfluidic reactors are devices known for their smaller dimensions, large surface-to-volume ratios, and well-defined reaction times. Enzymes immobilized in such microfluidic reactors can exhibit distinct benefits, such as fast reaction rate, high storage stability, suppressed autolysis, and ease of use. The use of microfluidic immobilized enzyme reactors (μ -IMERs) offers several advantages over traditional technologies in performing biocatalytic reactions, such as low energy consumption, rapid heat exchange, fast mass transfer, high efficiency, and superior repeatability. In this review, the strategies of employing μ -IMERs for continuous biocatalysis have been investigated via a top-down approach. First, from the macroscopic perspective, the fabrication techniques of microfluidic reactors are presented encompassing materials, configurations, and technologies. Then, from the microscopic point of view, several strategies are discussed for the internal structural designs of microfluidic reactors. Moreover, when we move to the nanoscopic level, attention is paid to the choice of enzyme immobilization techniques for performance enhancement. Finally, the scalability of microfluidics that transfers biocatalysis from laboratory to industrial production was investigated. This review is intended to provide a guideline for using biocatalysis in microreactors and expediting the progress of this important research area.

Received 3rd June 2019,
Accepted 16th September 2019

DOI: 10.1039/c9re00217k

rsc.li/reaction-engineering

1. Introduction

Biocatalysis is regarded as the most important green research area for sustainable manufacturing in the pharmaceutical and fine chemicals industries due to its low operating costs and high eco-efficiency.¹ Enzymes are an important type of natural catalyst used for biocatalysis, which exhibit several excellent characteristics that are lacking in artificial catalysts, such as high efficiency, enhanced selectivity, environment-friendly, and ability to catalyze a reaction under milder conditions.² The applications of enzymes for green and sustainable chemical synthesis in the industry have also infiltrated into our daily life. Despite this, certain aspects of enzymes still need to be improved upon prior to their

applications in the mass production of industrialized products, such as reusability and activity recovery for economic effects, long-term operation and storage stability, inhibition of certain reaction products, and selectivity toward nonnative substrates.³ Moreover, the separation of enzymes from products after the completion of a reaction, although incurs time and effort, is always an indispensable part of

^a Department of Applied Physics, The Hong Kong Polytechnic University, Hong Kong, China. E-mail: apzhang@polyu.edu.hk

^b The Hong Kong Polytechnic University Shenzhen Research Institute, Shenzhen, China

^c State Key Laboratory of Analog and Mixed Signal VLSI, Institute of Microelectronics, University of Macau, Macau, China

^d Department of Electrical and Electronic Engineering, Southern University of Science and Technology, Shenzhen, China

^e Faculty of Science and Technology, University of Macau, Macau, China

^f Faculty of Health Sciences, University of Macau, Macau, China



Yujiao Zhu

Yujiao Zhu received her B.Eng. in Materials Science and Engineering from the University of Science and Technology, Beijing, in 2014, and PhD in Applied Physics from the Hong Kong Polytechnic University in 2019. She is currently a Research Assistant in the Hong Kong Polytechnic University and University of Macau. Her research interests are bio-microfluidics, artificial photosynthesis, and green energy.

work. The possible contamination of products should be avoided and the overall operational costs could be reduced.⁴ Fortunately, enzyme immobilization is an impressive way to overcome these drawbacks. It considerably simplifies the separation and recovery of enzymes. The activity, stability, and selectivity of enzymes can also be improved after immobilization.⁵ Researchers have devoted considerable effort toward studying various enzyme immobilization techniques so far, including physical adsorption, affinity bonding, covalent binding, and encapsulation.^{6–9} Nevertheless, inappropriate immobilization can also cause conformational changes, blocking of active sites, and diffusion resistance to the enzyme, which, in turn, result in activity loss. Considering the structural diversity, complexity,

and variability of enzymes, as well as their sensitivity toward environmental conditions, the selection of immobilization techniques should be very careful with specific analyses. Further, the exploration of simple, efficient, and widely adaptable enzyme immobilization methods should get increased attention.

In laboratory studies involving enzyme immobilization, a higher yield can be obtained if the products are separated from the enzymes in time and the substrates are continuously supplemented.¹⁰ Therefore, the application of enzyme immobilization in continuous microfluidic reactors has attracted huge interest in industrial production, such as the syntheses of petrochemicals, active pharmaceutical ingredients, and value-added materials.^{11–13} Continuous



Qingming Chen

Polytechnic University. His research interests mainly focus on optofluidics, lab-on-a-chip systems, and optical devices.

Qingming Chen received his BSc in optical information science and technology from the Huazhong University of Science and Technology, Hubei, China, in 2011, M.Eng. in optical engineering from Jinan University, Guangdong, China, in 2014, and PhD in applied physics from the Hong Kong Polytechnic University, Hong Kong, in 2018. Since 2018, he has been a Postdoctoral Research Fellow with Hong Kong



Li-Yang Shao

University of Science and Technology (SUST). In 2018, he became the Associate Dean of the School of Innovation and Entrepreneurship in SUST. His research interests include fiber grating, sensors, and smart sensing systems for the railway industry.

Li-Yang Shao received his PhD degree in Optical Engineering in 2008 from Zhejiang University. He was a research assistant/associate at the Hong Kong Polytechnic University (HKPU) from 2006 to 2009. Then, he worked as a Postdoctoral Fellow successively at Carleton University, HKPU, and University of Sydney. In 2013, he joined the Southwest Jiaotong University as a Professor. In 2017, he joined the Southern



Yanwei Jia

Assistant Professor in the State Key Laboratory of Analog and Mixed Signal VLSI (AMSV), University of Macau, leading a group working on microfluidics for biological/chemical applications.

Yanwei Jia received her PhD, MSc, and BSc degrees in Physics from the National University of Singapore (2006) and Hunan University in China (2002 and 1996), respectively. After her PhD, Jia worked as a Research Fellow in the National University of Singapore in 2006 before she moved to Brandeis University in the USA, working as a Postdoctoral Fellow, Research Associate, and Research Scientist (2006–2012). She is currently an



Xuming Zhang

Xuming Zhang is currently an Associate Professor with the Department of Applied Physics, the Hong Kong Polytechnic University. He received his B. Eng. degree in Precision Mechanical Engineering from the University of Science & Technology of China (USTC) in 1994, and his PhD from the School of Electrical & Electronic Engineering, Nanyang Technological University (NTU) in 2006. His research resulted in more than 100 journal papers with an h-index of 28 and citation count of 2900. His current research interests mainly include microfluidics, artificial photosynthesis, biomimetics, and green energy.

microfluidic systems outperform batch systems accompanied by several advantages, such as smaller dimensions, low cost and energy consumption, high efficiency, rapid heat exchange, and fast mass transfer.^{14–16} In particular, a large surface-area-to-volume (SAV) ratio for microfluidic reactors is advantageous for enzyme loading. Different microchannel types (*e.g.*, wall-coated type, packed-bed type, and monolithic type) also provide various possibilities for the integration of immobilization carriers into the micro space. When the enzyme is immobilized in microfluidic reactors, there is no need to separate the enzyme-loaded carriers from the reaction solution, which facilitates the recovery and reusability of the enzyme, therefore saving time and labor. Moreover, different catalytic reaction conditions (such as temperature, pH, residence time, and pressure) are easier to control in microfluidic reactors as compared to operation in batch systems.¹⁷ Higher temperature with low-boiling solvents, higher pressure, more uniform heat/pressure distribution, safer and easier reaction control, and less unwanted products can be achieved.¹⁸ Furthermore, reaction stoppages can be easily achieved by pumping the substrate out of the reactors without the need for the addition of an acid or base that may affect the detection accuracy or products. Further, microfluidic reactors can be directly incorporated into many instruments for real-time analysis and monitoring. Moreover, many natural biocatalytic reactions are cascaded multienzyme reactions.¹⁹ Immobilizing enzymes in microfluidic reactors facilitate control over their sequential order and relative positions, thereby reverting to natural cascaded reactions to the maximum extent. In addition, microfluidic reactors are easily scaled up or scaled out once careful design factors are taken into account.²⁰ In general, these promising features of continuous microfluidic immobilized enzyme reactors (μ -IMERs) hold the key for their application in green, sustainable, economical, and large-scale industrial production.^{21–23}

This review provides a comprehensive discussion on the factors that affect the performance of continuous biocatalysis in μ -IMERs using a top-down strategy. From the macroscopic point of view, the first thing to consider is the fabrication of microfluidic reactors in addition to materials' and configuration designs. Various materials have been developed in microfluidics, such as silicon, glass, polymers, and paper. The characteristics of fabrication materials are of vital importance to the performance of catalytic reactions. Special biocatalysis can also be achieved with a careful design of the device configuration. From the microscopic point of view, the capacity of the inner structures of the microreactors for enzyme loading also plays a significant role in the overall biocatalytic efficiency. In addition, the specific substrate diffusion path induced by different types of microreactors should also be taken into account. Moreover, from the nanoscopic point of view, different immobilization techniques, which dominate the performance of enzymes (*e.g.*, activity, stability, and reusability) in the

nanoenvironment of biocatalytic reactions, are also comprehensively studied. Finally, the scalability of microfluidics that can facilitate the transfer of biocatalysis in the laboratory to that in the industry for large-scale production is briefly reviewed. We hope that the discussion in this review can facilitate the understanding of the main characteristics of the rapidly developing μ -IMERs field that can be used to undertake continuous biocatalysis and can provide a clear guideline for future research.

2. Engineering of microfluidic reactors

2.1 Materials for microfluidic reactors

There are many materials that have been used for the fabrication of microfluidic reactors. The basic characteristics are stability and inertness.²⁴ In the early days, silicon²⁵ and glass were mostly used, which were directly inherited from the semiconductor industry and microelectromechanical systems (MEMS).²⁶ They usually require surface salinization and the introduction of certain functional groups such as carboxyl groups or amino groups for further immobilization;²⁷ however, high cost and complicated fabrication procedures usually limit their applications in microfluidics. Therefore, several polymers with easy fabrication and high compatibility for biocatalysis have become fairly popular for use in microfluidics.

As a typical silicon-based organic polymer, polydimethylsiloxane (PDMS) has been very popular in biomicrofluidic applications. Its advantages are excellent biocompatibility, easy fabrication, low cost, and optical transparency, which are beneficial for the monitoring and optical detection of biocatalytic reactions.²⁸ The flexibility feature also makes PDMS an excellent material to fabricate valves and pumps in microfluidic devices. Nevertheless, certain problems of PDMS are not negligible: swelling in certain organic solvents, changes in solution concentrations due to water evaporation, and hydrophobic surfaces that lead to nonspecific adsorption of biomolecules. Therefore, oxygen plasma or surface modification is usually required to make it hydrophilic and to introduce functional groups for enzyme immobilization.

Other polymer materials, such as polymethyl methacrylate (PMMA),^{29–31} polystyrene (PS),³² polycarbonate (PC),³³ poly(ethylene terephthalate) (PET),³⁴ and polytetrafluoroethylene (PTFE),^{35,36} have also been widely used for microfluidics fabrication. Although they possess excellent chemical, electrical, mechanical, optical, and thermal properties,^{37–40} they usually require additional surface modifications due to the lack of functional groups on the surfaces. Sometimes, stainless steel and ceramics are used for reactor fabrication if the reaction is operated under higher temperatures and higher pressures.⁴¹ However, their high fabrication cost largely restricts their broader applications. Ogończyk *et al.* firstly used PC microchannels for enzyme immobilization in 2012.³³ The PC microfluidic chip could immobilize different kinds of enzymes, such as

alkaline phosphatase (ALP) and urease, by the physical-chemical method. Further, enzymatic microfluidic chips also exhibit attractive operation reproducibility, storage stability, and higher conversion rates.

Paper is another promising material for the fabrication of microfluidic reactors. Paper-based microfluidics generally have porous and open channels, which provide larger surface areas for enzyme immobilization as compared to conventional microfluidics, which only have hollow channels. However, paper-based microfluidics are mainly used for biochemical analysis, medical diagnostics, and forensic diagnostics,^{42,43} which are not in the scope of this review.

2.2 Configuration design of microfluidic reactors

The configuration of microfluidic reactors varies under different situations. Four representative configuration designs are shown in Fig. 1. A single-channel microfluidic chip is the simplest. It has only one straight channel for the immobilization of enzymes and substrate transport (Fig. 1a). Open-tubular capillaries can also be classified under this category. Nevertheless, the volume of such a chip is generally limited for enzyme loading. A serpentine channel (or curved channel) is accordingly designed by folding up a single channel into a serpentine (curved) shape to increase the effective volume for immobilization (Fig. 1b). A multichannel microfluidic chip is a more advanced design that multiplies the effective immobilization volume.⁴⁴ As shown in Fig. 1c, the microchannels are divided into an array on the input side and a similar unit on the output side. For further volume increase, a planar microfluidic chip is presented by simply enlarging the channel into a planar chamber in the lateral direction (Fig. 1d).

The configuration of microfluidic reactors should be well designed when applied to continuous biocatalysis. In the bulk system, the substrate solutions react with enzymes by mixing and diffusion. The reaction performance is unlikely influenced by the container shape. However, in a microfluidic chip, the substrate solutions are driven by external forces to react with enzymes immobilized on the chip. If the

immobilization amount of the enzyme and residence time of biocatalysis are fixed, the configuration design can have a substantial impact on the accessibility of the substrate to the immobilized enzyme, which then affects the overall biocatalytic reaction performance.⁴⁵ Hoffmann *et al.* designed four HRP-immobilized microreactors with different configurations: full surface, half surface, fine checkerboard, and coarse checkerboard.⁴⁵ Fig. 2a shows product absorbance at the reactor outlet for each pattern. The fine and coarse checkerboard structures exhibit an increased efficiency, with 81% and 56% higher absorbance per active area than the fully modified surface. Different configurations can yield different velocities across the reactors, thereby influencing mass transport and fluid mixing. Consequently, the accessibility of the substrate for the enzyme near the surface is affected, leading to a difference in the reaction performance.

Further, Nakagawa *et al.* proved that the channel shape has a substantial impact on the backpressure, which further affects enzyme activity.⁴⁶ Five microreactors with different numbers and lengths of elbows and straight sections were prepared. Protease was immobilized in a freeze-dried polyvinyl alcohol (PVA) micromonolith prepared in the microreactors. The proteolytic reaction yields of the five reactors obtained under the same residence time were significantly different due to the changes in the elbow and straight sections, as shown in Fig. 2c–g. The microreactor with the least number of elbow sections had the highest reaction yield, but the smallest pressure drop (Fig. 2h). The pressure drop is related to the resultant fluid resistance, which is determined by microchannel patterning. Therefore, the accessibility of the substrate to the immobilized enzyme *via* diffusion is largely affected, resulting in differences in the reaction yields. Then, the microreactor with the smallest pressure drop would have the highest enzyme activity.

2.3 Fabrication technologies of microfluidic reactors

The fabrication process of microfluidic reactors includes microchannel fabrication and microfluidic chip bonding.

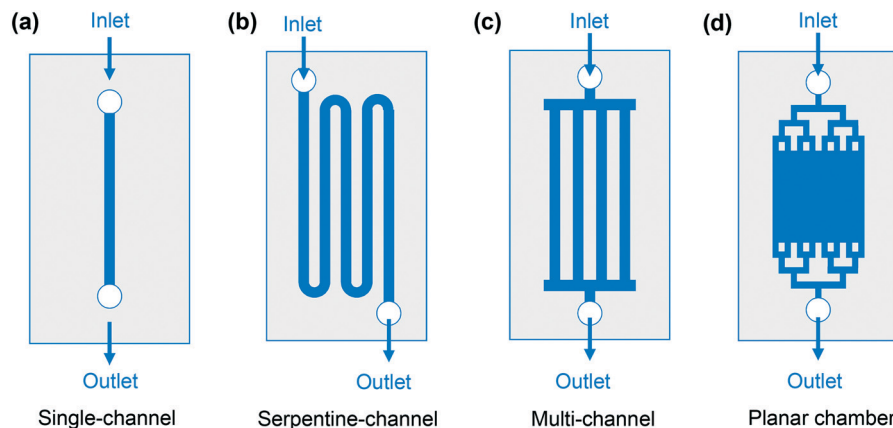


Fig. 1 Representative configuration designs of microfluidic chips: (a) single-channel chip, (b) serpentine-channel chip, (c) multi-channel chip and (d) planar chamber chip.

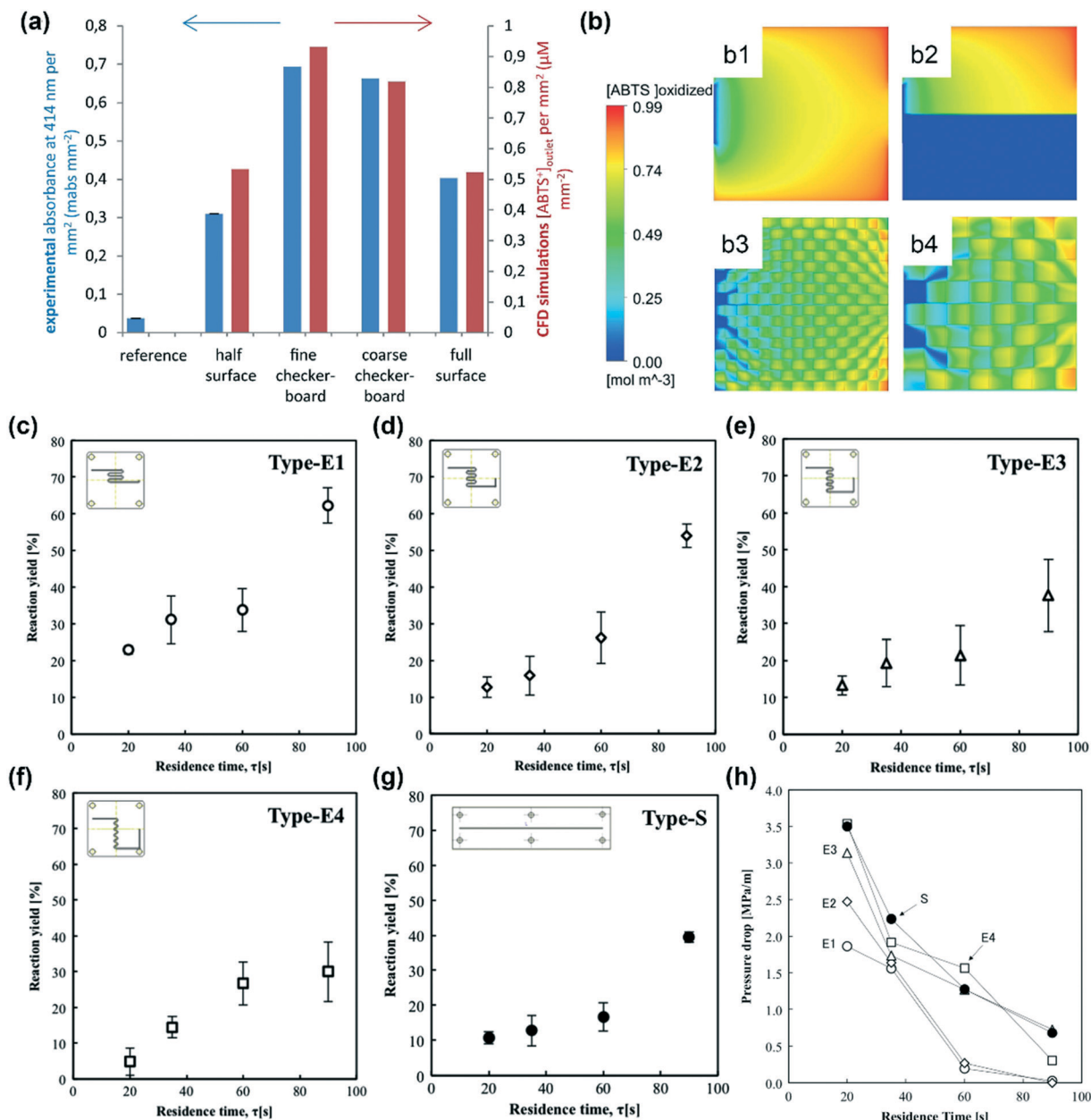


Fig. 2 (a) Comparison of experimentally determined ABTS⁺ absorbance at 414 nm for per mm² of the modified area at the reactor outlet under the steady-state condition (blue) and ABTS⁺ outlet concentration obtained from CFD simulations in mM mm⁻² (red) for the different surface patterns: reference (horseradish peroxidase (HRP) adsorption on a nonmodified surface; empty squares), half-modified surface, coarse checkerboard, fine checkerboard, and fully modified surface; (b) illustrations of the product concentrations on the top surface of the microreactor (under steady-state simulations) dimensions using the fully modified surface (b1), half-modified surface (b2), fine checkerboard structure (b3), and coarse checkerboard structure (b4), where the red surfaces illustrate high and blue surfaces denote low product concentrations. These two figures were reproduced from ref. 45 with the permission from Elsevier Ltd. (c)–(g) Reaction performances of the five prepared reactors using 0.1% β -lactoglobulin solution as the substrate. (h) Pressure drops of the five prepared reactors. These 6 figures were reproduced from ref. 46 with permission from Elsevier Ltd.

The techniques for both these steps should be carefully selected by considering the reactor material, reactor configuration, and fabrication cost and time. For microchannel fabrication, most techniques are adopted and improved from the MEMS, such as photolithography, etching, soft lithography, thermoforming, and so on. In contrast, the techniques for the bonding process are

generally different from those used in MEMS. They may be divided into indirect and direct bonding.

2.3.1 Microchannel fabrication. The most widely used technique to fabricate silicon/glass microfluidic channels is photolithography, where the pattern of a photomask is transferred to the substrate with the assistance of a photosensitive resist. It comprises six steps, as shown in

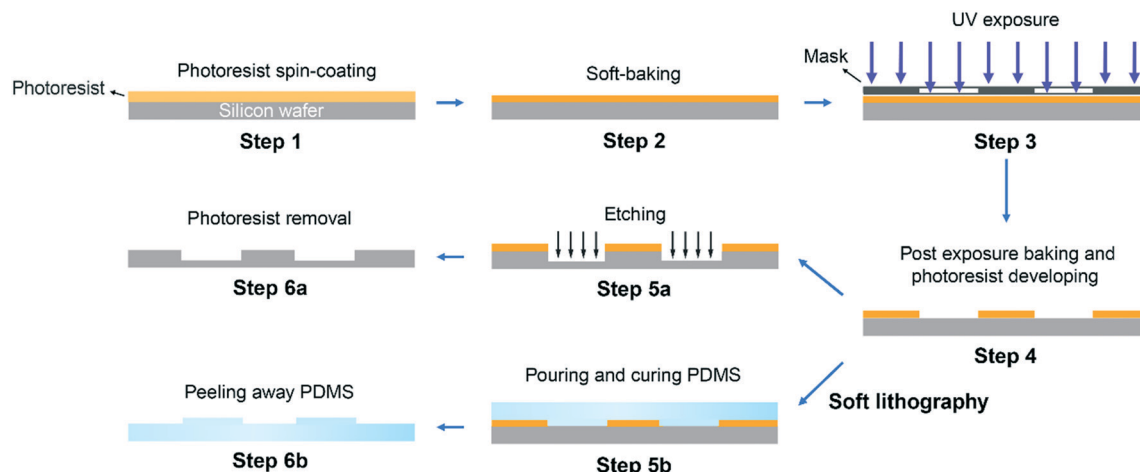


Fig. 3 Process flow of photolithography and soft lithography with PDMS.

Fig. 3. Step 1: the photoresist is spin-coated onto a thoroughly cleaned wafer to form a thin layer. Step 2: the wafer is soft-baked to remove the solvents in the photoresist and improve the adhesion of the resist to the wafer. Step 3: the photoresist layer is exposed to UV light with a photomask. Step 4: the photoresist layer is then immersed in a developer solution to generate a mask for etching following post-exposure baking. Step 5a: microchannels are formed on the substrate by etching to remove the unprotected areas of the photoresist mask. Step 6a: the microchannels are ready for use after the residual photoresist is removed.

As an extension of photolithography, soft lithography is a collection of techniques to fabricate microstructures in a wide range of soft elastomer materials, such as polymers, gels, and organic monolayers for microfluidic applications.⁴⁷ Basically, it uses a patterned elastomeric polymer layer as a mask, mold, or stamp to emboss, mold, or print the pattern to another soft substrate.⁴⁸ The patterned elastomeric polymer is usually a layer of PDMS that is fabricated from a solid master produced by photolithography (as shown in steps 5b and 6b, Fig. 3). The basis of soft lithography includes microcontact printing, replica molding, micro-transfer molding, micromolding in capillaries, and a large number of patterning techniques.⁴⁹

Thermoforming techniques are usually employed to pattern semifinished thermoplastic foils by stretching or stamping with pressure and heat.^{50,51} Injection molding and hot embossing can also be classified in this category. They have the advantages of cost-effective high-volume fabrication and high-frequency manufacturing.⁴⁴ However, thermo-forming techniques are less precise for controlling the aspect ratio than lithography techniques.⁵²

2.3.2 Bonding process. The bonding process is a very critical step subsequent to microchannel fabrication, where microfluidic reactors are sealed to form enclosed fluid paths.^{53,54} Indirect bonding uses an adhesive layer to bring two substrates together. Generally, epoxy, adhesive tapes, or chemical reagents are used. The additional layer may affect

the chemical, optical, and mechanical properties of the substrate materials. In contrast, the direct bonding method, such as oxygen plasma bonding, allows sealing without any additional materials to the interface.⁵⁵ As a result, the sidewalls of the microchannels would be homogeneous with the substrates. The effect of the bonding process to the properties of the substrates should be carefully considered when selecting the bonding method. Moreover, certain other key parameters, such as bond strength, surface chemistry, material properties, and fabrication costs, should also be taken into account.

2.3.3 Three-dimensional printing for microfluidics. PDMS and soft lithography make the fabrication of microfluidics easy and cost-effective.⁵⁶ However, the limitations of these traditional techniques for microfluidics on the large scale, mass production, and fabrication of three-dimensional (3D) structures are still inescapable. Recently, the application of 3D printing in microscale fabrication has attracted considerable interest in microfluidics due to the rapid development of commercial 3D printers.⁵⁷ 3D printing has the obvious advantages in rapidly fabricating complex 3D microfluidic devices in a single step from a computer model.⁵⁸ The most widely used 3D printing techniques include selective laser sintering (SLS), fused deposition modeling (FDM), photopolymer inkjet printing, laminated object manufacturing (LOM), and stereolithography (SL).⁵⁶ Nevertheless, fabricating microfluidic devices using the 3D printing technology still needs attention toward certain aspects, such as precise control at the smaller scale, cost reduction, and adaptability of 3D printers to different materials.^{59,60}

3. Internal structural designs of microfluidic channels

The amount and activity of immobilized enzymes in a microfluidic chip can considerably impact the biocatalytic reaction rate. Further, the internal structure of microfluidic

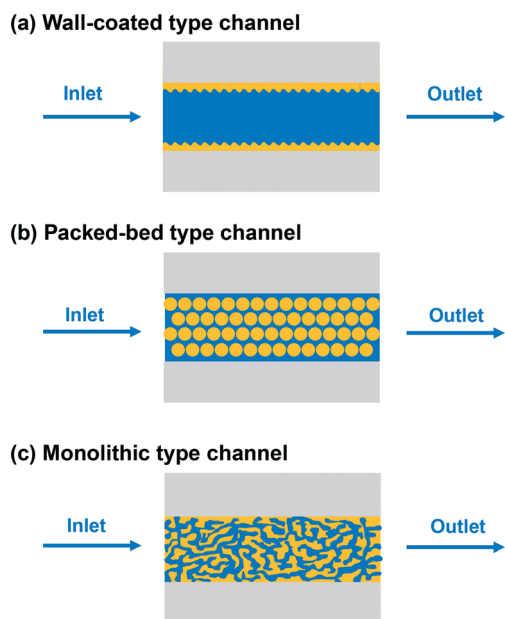


Fig. 4 Typical designs for the internal structure of microfluidic channels: (a) wall-coated type channel, (b) packed-bed type channel and (c) monolithic type channel.

channels can strongly affect these two factors that can be achieved by adjusting the SAV ratio of the microchannel and the diffusion pressure of the solution passing through it. Generally, the internal structures of μ -IMERs are classified into three types: wall-coated type, monolithic type, and packed-bed type (Fig. 4). A comparison of the properties of these three types of microchannels is provided in Table 1.

3.1 Wall-coated-type channel

For wall-coated-type μ -IMERs (Fig. 4a), the enzyme is directly immobilized onto the inner wall of the microchannel.^{61–63} Notably, the available surface areas of the microfluidic walls are fairly limited, resulting in low enzyme-loading capacity. In addition, the substrate diffusion path is relatively large in this case, leading to a low biocatalytic conversion rate. Researchers have been dedicated toward increasing the SAV ratio of microchannels, thereby enhancing the enzyme-loading capacity. One efficient method to achieve this is to modify the inner wall with certain biocompatible nanostructured materials such as dopamine,⁶⁴ gold nanoparticles,⁶⁵ graphene,^{66,67} graphene oxide,^{68,69} nanosprings,⁷⁰ or MXenes.⁷¹

Table 1 Comparison of the properties of different microchannel types

Microchannel type	Wall-coated	Packed-bed	Monolithic
SAV ratio	Small	Large	Large
Pressure drops	Low	High	Low
Diffusion length	Large	Small	Small
Heat transfer	Large	Small	Moderate
Mechanical stability	High	Low	Moderate

Recently, Valikhani *et al.* designed a borosilicate microchannel with silica nanosprings attached to the surface for the immobilization of sucrose phosphorylase (Fig. 5a).⁷⁰ It has been demonstrated that the enzyme-loading amount can be increased by an order of magnitude or more as compared to that of enzyme loaded on uncoated microchannel walls. Moreover, nanospring microreactors showed enhanced conversion efficiency involving the synthesis of α -glucose-1-phosphate and improved reusability and stability when compared with a plain microreactor. Another feasible solution to increase the active enzyme-loading amount is to multiply the immobilization layers, which is also referred to as the layer-by-layer (LBL) assembly approach.^{34,35,72–74} A representative work was conducted by Bi *et al.* who alternatively absorbed polyethyleneimine (PEI) and *Candida antarctica* lipase B (CAL-b) on the microreactor surface (Fig. 5b).³⁵ Lipase loading was enlarged as the number of layers increased. It reached saturation at the eighth layer. The microreactor was also demonstrated to have high conversion efficiency and excellent stability for producing wax ester.

3.2 Packed-bed-type channels

Even though many methods have been developed to increase the SAV ratio of wall-coated-type μ -IMERs, the room for enhancement is very small. In order to maximize the space utilization of size-limited channels and therefore maximizing the enzyme-loading amount, enzymes are designed to be immobilized on polymeric or inorganic particles. The enzyme-immobilized particles are then packed into the microchannel of μ -IMERs, which is regarded as a packed-bed-type channel (Fig. 4b). The higher SAV ratios of a packed-bed channel also ensure relatively shorter diffusion distances between substrates and enzymes when compared with those in wall-coated channels.^{75,76} Many polymeric particles have already been commercially available for packing.^{76–79} Certain inorganic materials such as glass,^{80,81} silica,⁸² and Fe_2O_3 microparticles^{83–85} have also been explored. These packed-bed-type μ -IMERs can be easily fabricated and exhibit an extremely high enzyme-loading capacity.

Kundu *et al.* designed a microreactor packed with commercially available mesoporous PMMA beads, where CAL-b was physically immobilized to study the polymerization of polycaprolactone from ϵ -caprolactone in the continuous mode (Fig. 6a–c).⁷⁷ It was demonstrated that faster polymerization and higher molecular mass could be obtained in the microreactors as compared to that in the batch reactors. Another example is the packing of GOx-modified MNPs in microfluidic channels for the electrochemical detection of glucose (Fig. 6d).⁸⁵ The performance of MD could be optimized by changing the packing length of MNPs, which was difficult to achieve in other types of devices. The device also showed good reproducibility, favorable stability, and promising potential

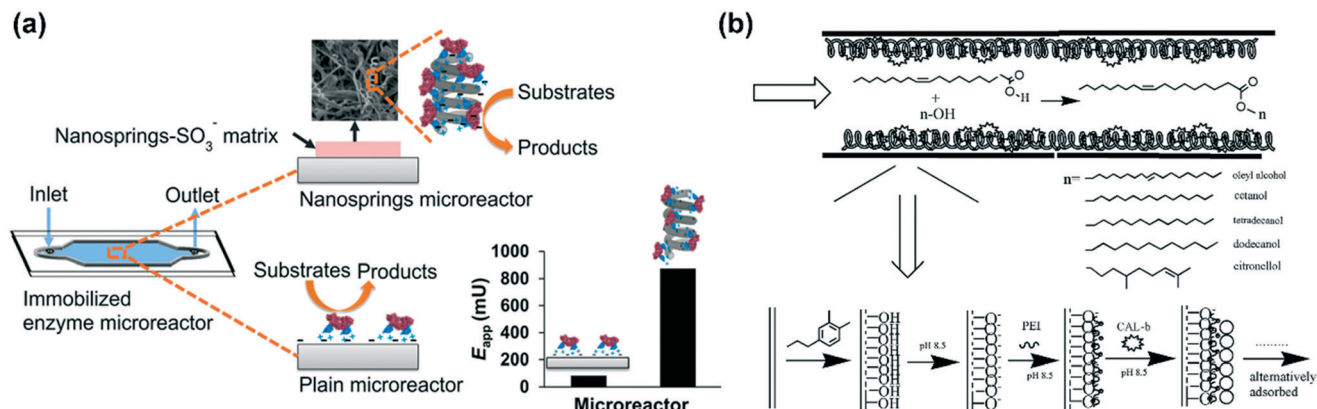


Fig. 5 Examples of wall-coated microchannels for enzyme immobilization. (a) Schematic of sucrose phosphorylase immobilized on nanospring microreactors with enhanced enzyme activity. Reprinted with permission from ref. 70. Copyright 2017 American Chemical Society. (b) Process of immobilization of CAL-b based on the self-oxidation of dopamine and LBL method. Long chains with positive charges represent PEI, and circles represent lipase. Reproduced from ref. 35 with permission from The Royal Society of Chemistry.

in glucose detection without the need for pretreatment of serum samples. However, due to the densely packed particles, the fluid passing through the channel is difficult to control and heat transfer inside the channel is very limited.⁸⁶ Moreover, there may be substantial pressure drops when the substrate solution flows along the channel. These may negatively impact the enzyme activity.

3.3 Monolithic-type channel

To overcome the drawbacks of a packed-bed-type channel, such as high pressure drops, limited heat transfer, and possible leakage at higher flow rates, a monolithic-type channel (Fig. 4c) has been developed. In such a case, the channel is filled by monolithic material with interconnected meso- or microporous structures. Such a structure exhibits higher void fractions, facilitating fluid flow. Consequently, relatively higher flow rates, lower pressure drops, and higher

productivities can be achieved as compared to those obtainable from packed-bed-type channels in monoliths.^{1,87-89} Higher backpressure can facilitate the rapid diffusion of substrate to the immobilized enzyme. As a result, the enzyme activity is increased, which is reflected from an increase in the turnover number (k_{cat}) and decrease in the Michaelis constant (K_M).⁹⁰ It also possesses the advantages of high mechanical durability and reduced diffusion path length over a wall-coated-type channel. Qiao *et al.* immobilized L-asparaginase (L-ASNase) in both monolithic microreactor and coated reactor (*i.e.*, the wall-coated type) by the same immobilization method.⁹¹ Fig. 7a-d show the SEM images of monolithic and coated microreactors. The monolithic microreactor was demonstrated to have lower K_M than that of the coated microreactor, showing that better affinity between the substrate and enzyme can be obtained in monolithic structures as a result of the lower diffusion path length in monoliths (Fig. 7e). However, a higher maximal

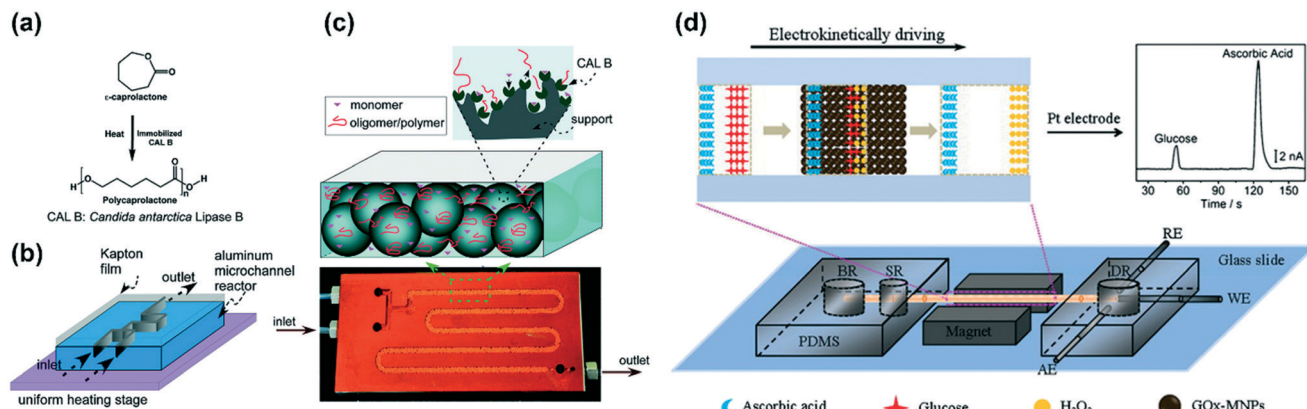


Fig. 6 Examples of packed-bed microchannels for enzyme immobilization. (a) Reaction scheme for ring-opening polymerization of ϵ -caprolactone to polycaprolactone. (b) Schematic of the microreactor setup. (c) Photograph of a typical microreactor used in this study. CAL-b-immobilized solid beads (macroporous PMMA) were filled in the channel. These three figures were reprinted with permission from ref. 77. Copyright 2011 American Chemical Society. (d) Schematic representation of the construction and analytical procedure of glucose oxidase (GOx)-magnetic nanoparticles (MNPs) microfluidic device (MD). BR: buffer reservoir; SR: sample reservoir; DR: detection reservoir; WE: working electrode; RE: reference electrode; AE: auxiliary electrode. Reproduced from ref. 85 with permission from Elsevier Ltd.

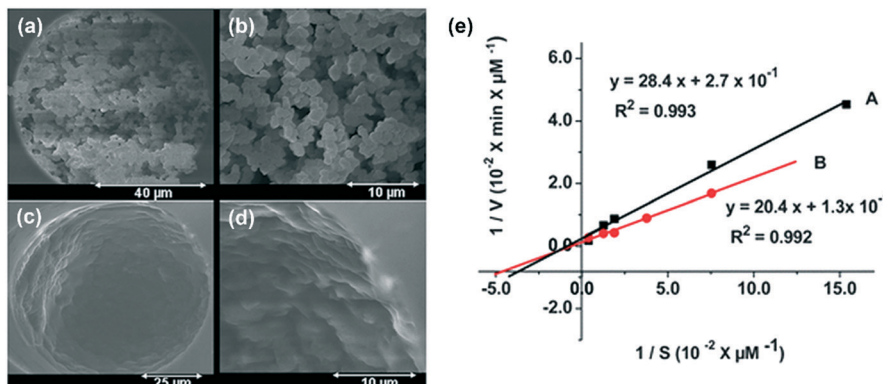


Fig. 7 SEM images of monolithic and coated microreactors in capillary: (a and b) monolithic, (c and d) coated. (e) Lineweaver–Burk plots of L-ASNase immobilized on monolithic (A, ■) and coated (B, ●) enzymatic microreactors. Reproduced from ref. 91 with permission from The Royal Society of Chemistry.

velocity was observed in the coated microreactor due to its relatively lower flow pressure.

The monolithic materials can be organic,^{92–96} inorganic,^{97–100} or hybrid.^{66,101–103} This selection should be carefully made for different enzyme immobilizations and different reaction environments. Generally, organic monoliths are copolymerized from many monomers; sometimes, one of the monomers is an enzyme. They usually have good biocompatibility and pH resistance, but may be damaged by certain organic solvents. An example is the immobilization of amylase in PVA foam by mixing an amylase solution with the PVA solution before they were put in a cylindrical sample case for freeze-drying.⁹³ The amylase-immobilized microreactor was demonstrated to successfully conduct continuous starch hydrolysis reactions over 8 days. For inorganic monoliths, silica-based monoliths are the most widely used due to their higher binding capacity, promising biocompatibility, chemical and thermal stabilities, and easy functionalization.¹⁰⁴ However, when compared with organic polymer monoliths, the preparation of inorganic monoliths is relatively difficult.¹⁰⁵ Therefore, monoliths used for enzyme

immobilization are mostly hybrids of organic and inorganic materials. For example, Ma *et al.* developed an organic-inorganic-hybrid silica monolith with immobilized trypsin and demonstrated its excellent enzyme activity and long-term stability in proteome analyses.¹⁰¹ However, there is still the possibility that the pores are blocked, leading to nonuniform permeability along the channel. Further, the fabrication of monolithic materials is usually time-consuming and poorly reproducible. Each portion of the internal structure has its own advantages and disadvantages. All the aspects should be taken into account as much as possible when designing the structure. In particular, attention should be paid to economy, sustainability, and green chemistry for industrial applications.

4. Enzyme immobilization techniques

Since Nillson and Griffin in 1916 firstly reported that invertase retained its activity after physical adsorption onto charcoal,¹⁰⁶ various enzyme immobilization techniques have been developed and studied. Most of these techniques can be

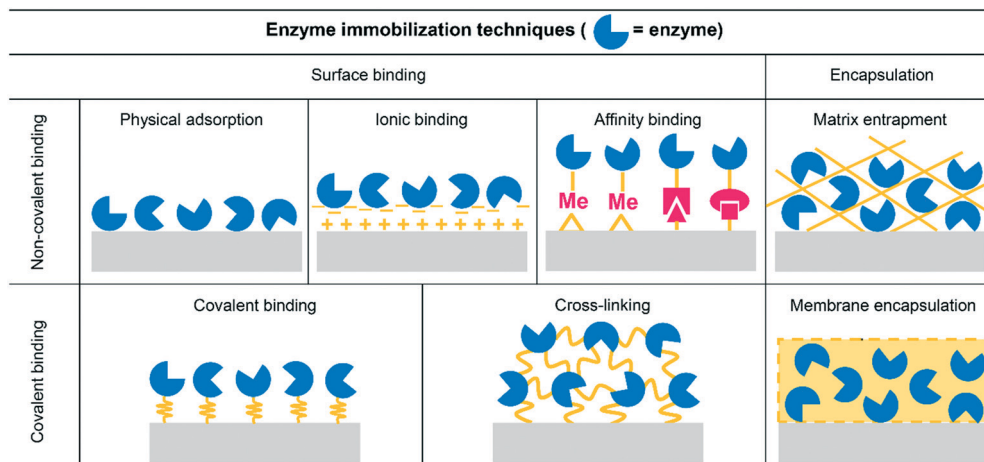


Fig. 8 Different enzyme immobilization techniques.

directly used for enzyme immobilizations in microfluidic chips for biocatalysis. A combination of enzyme immobilization and microfluidic chips provides the advantages of higher stability and reusability, high enzyme-to-substrate ratio, and rapid catalytic reactions.¹⁰⁷ Basically, the techniques of enzyme immobilization in microfluidic chips can be classified into two types: surface binding and encapsulation, as shown in Fig. 8. The inner surfaces of microfluidic reactors can offer support for enzyme immobilization when the surface binding technique is used. Moreover, microchannels with special microstructures can entrap relatively larger structures; then, the encapsulation of enzymes can be employed. For the surface binding method, it is usually subdivided into noncovalent binding and covalent binding. Noncovalent binding includes nonspecific physical adsorption, ionic bonding, His-tag/metal binding, and affinity binding.^{3,108} However, covalent binding involves the immobilization of enzymes on the surface *via* covalent forces between certain functional groups, such as amino, carboxyl, hydroxyl, or sulfhydryl groups.¹⁰⁹ With regard to encapsulation immobilization, enzymes are confined into smaller spaces built by polymeric networks, membranes, or nanochannels. Different immobilization methods have different advantages as well as disadvantages (see Table 2). Therefore, careful consideration should be made before any immobilization strategy is adopted. Some representative examples of μ -IMERs for biocatalysis are summarized in Table 3.

4.1 Surface binding

4.1.1 Nonspecific physical adsorption. Nonspecific physical adsorption is the simplest and most convenient approach. The interactions between the enzyme and support are nonspecific forces, such as van der Waals forces, hydrogen bonds, and hydrophobic interactions.²⁷ When compared with other immobilization methods, the conditions for physical adsorption are milder and no chemical modification is needed during the procedures. Therefore, the chances of conformational changes caused by immobilization are marginal. In addition, physical adsorption is usually reversible, making it possible for the same device to be reused by washing and reloading new

enzymes. This indicates a relatively low fabrication cost for large-scale production.³

However, nonspecific forces are generally very weak and highly dependent on environmental and surface conditions. As a result, enzymes can easily fall off from the surface, particularly in fluidic systems or high ionic and pH solutions. This would cause the contamination of reaction systems and reduction of enzyme activity. In addition, since the enzymes adsorbed on the support are randomly oriented, the activity of enzymes can also be affected by the hindering of active sites to the support due to the random orientation after adsorption. Moreover, certain other problems, such as diffusion resistance, denaturation of enzyme, and overloading, could also cause enzyme activity loss when physical adsorption is adopted.¹²¹ Therefore, a combination of other immobilization methods with the adsorption method is usually applied to overcome these shortcomings and to enhance the enzyme activity, stability, and overall efficiency.

4.1.2 Ionic binding. Ionic binding is achieved by electrostatic interactions between the positively and negatively charged functional groups of the enzymes and supports. The amount of immobilized enzyme can be effectively manipulated if the pH of the solution is controlled below the isoelectric point of the enzyme and above that of the support material.¹⁰⁴

Generally, ionic binding is stronger than nonspecific physical adsorption, which can subsequently guarantee higher enzyme stability and reusability. However, ionic binding is highly dependent on environmental pH and ionic strength. This may affect the enzyme-loading amount and pH stability of the enzymes. Therefore, the selection of suitable chemicals with an appropriate isoelectric point is the focus of this method. In biochemistry, typical positively charged functional groups are protonated amines (NH_3^+) and quaternary ammonium cations (NR_4^+). Negatively charged functional groups are usually carboxylic acid ($-\text{COO}^-$) and sulfonic acid ($-\text{RSO}_3^-$).²⁷ PEI is a popular polycation, which has multiple cation groups with strong anion exchange capacity for enzyme immobilization by ionic binding.^{35,122–125} Some other polycations have also been used for ionic binding, such as chitosan,^{34,72} hexadimethrine bromide (HDB),^{110,126} and poly(diallyldimethylammonium chloride)

Table 2 Characteristics comparison of different enzyme immobilization techniques

Characteristics	Physical adsorption	Ionic binding	Affinity binding	Covalent binding	Cross-linking	Entrapment and encapsulation
Preparation	Simple	Simple	Moderate	Difficult	Moderate	Difficult
Cost	Low	Low	Moderate	High	Moderate	Moderate
Applicability	Wide	Wide	Wide	Selective	Selective	Wide
Binding force	Weak	Moderate	Moderate	Strong	Strong	Strong
Stability	Low	Moderate	Moderate	High	High	High
Enzyme leakage	Yes	Possible	Possible	No	No	Possible
Enzyme activity	Moderate	High	High	Low	Low	Moderate
Protection from microbial	No	No	No	No	Possible	Yes
Diffusional limitation	Low	Low	Low	Low	Moderate	High

Table 3 Summary of recent μ -IMERs studies

Immobilization techniques	Enzyme	Platform	Biocatalysis performance	Ref.
Physical immobilization	CAL-b	Macroporous PMMA microbeads packed aluminum microreactor	Faster polymerization and higher molecular mass	77
Ionic binding	Angiotensin-converting enzyme	Fused silica capillary column	High activity, stability, reusability, renewability and reduced costs	110
	Sucrose phosphorylase	Nanosprings-coated Borosilicate glass	10-fold activity enhancement, 11-fold operational stability increase, 85% conversion rate retaining after 840 reactor cycles	70
Layer-by-layer ionic binding	Trypsin	Wall-coated PET microfluidic chip	Short digestion time and small volume of protein samples, a potential solution for low-level protein analysis	34
	CAL-b	PTFE open-tubular microreactor	Production efficiency reached to 95% within 35 min, 83% initial activity retained after 144 hours usage	35
His-tag/Ni-NTA binding	PikC hydroxylase	Agarose beads packed PDMS microfluidic reactor	High enzyme loading and conversion rate	111
	Transketolase	Wall-coated PMMA microfluidic chip	The 1-step-immobilization method without the pre-amination of PMMA surface showed higher specific activity	112
Streptavidin/biotin	ALP, GOx and HRP	Phospholipid bilayer-coated PDMS microchannels and borosilicate microcapillary tubes	The feasibility of using the microchannels to obtain kinetic data and the potential application for multistep chemical synthesis were demonstrated	113
	HRP and β -galactosidase	PDMS microchip reactor packed with commercial microbeads	Similar kinetic analysis results were obtained in the microfluidic-based assays as that obtained in solution, reduced cost, reagent economy and increased throughput were observed	79
	ALP, Gox and HRP	Protein coated PDMS/glass microchannel	Photoimmobilization of multiple, well-defined enzymes were developed for both single-enzyme and multi-enzyme systems	114
DNA directed immobilization	CAL-b and HRP	Fused silica capillaries with polymer coated	High reusability and renewability, the reaction time available for glucose oxidase could be independently and modularly varied by the distance between two enzymes	115
Covalent binding	Trypsin	Porous polymer monolithic microfluidic capillaries and chips	Very short digestion time compared to the traditional approach and great potential for broader application in various protein mapping	96
	GOx	Magnetic nanoparticles packed microreactor	Low detection limit of glucose, high reproducibility and storage stability, availability of direct detection of serum samples	85
	β -Gal and GOx	Au coated PDMS microfluidic chip	5 times of the reaction yield could be obtained if the gap distance decreased from 100 to 50 μ m	116
Encapsulation	Trypsin	PMMA microchip filled with sol-gel	Analytic time was shortened and operation stability was increased, digestion of protein with multiple cleavage sites and separation of digest fragments are applicable	117
	Trypsin	Titania and alumina sol-gel based PDMS microfluidic reactors	Short digestion time and increased operation stability	118
	Lipase	Mesoporous silica coated PDMS/glass microreactor	Higher activity compared to that in batch system	119
Cross-linking	Aminoacylase	Wall-coated PTFE microtubes	Higher stability against heat and organic solvents, applicable to various enzymes with low isoelectric points	36
Cross-linking/encapsulation	ALP and urease	PDMS microfluidic device with PEG-based hydrogel structures	Enzyme-catalyzed reactions were able to reach 90% conversion within 10 min	120

(PDDA).^{127,128} Sometimes, polyanions such as alginate,^{122,123} hyaluronic acid (HA),^{34,72} poly(Lys),³⁶ and functionalized graphene oxide⁶⁹ have also been employed to form multilayers to stabilize immobilization and to increase the enzyme-loading amount.

Certain schematic representations of enzyme immobilization by ionic binding *via* different polycations and polyanions

are shown in Fig. 9. The reversibility of enzyme immobilization by ionic binding is also an important advantage over other immobilization methods. The support surface can be washed without damage by simply changing the ionic strength of the environment. Then, new enzymes can be immobilized onto the same support. In this way, the microfluidic chip can be reused, thereby saving labor and cost.

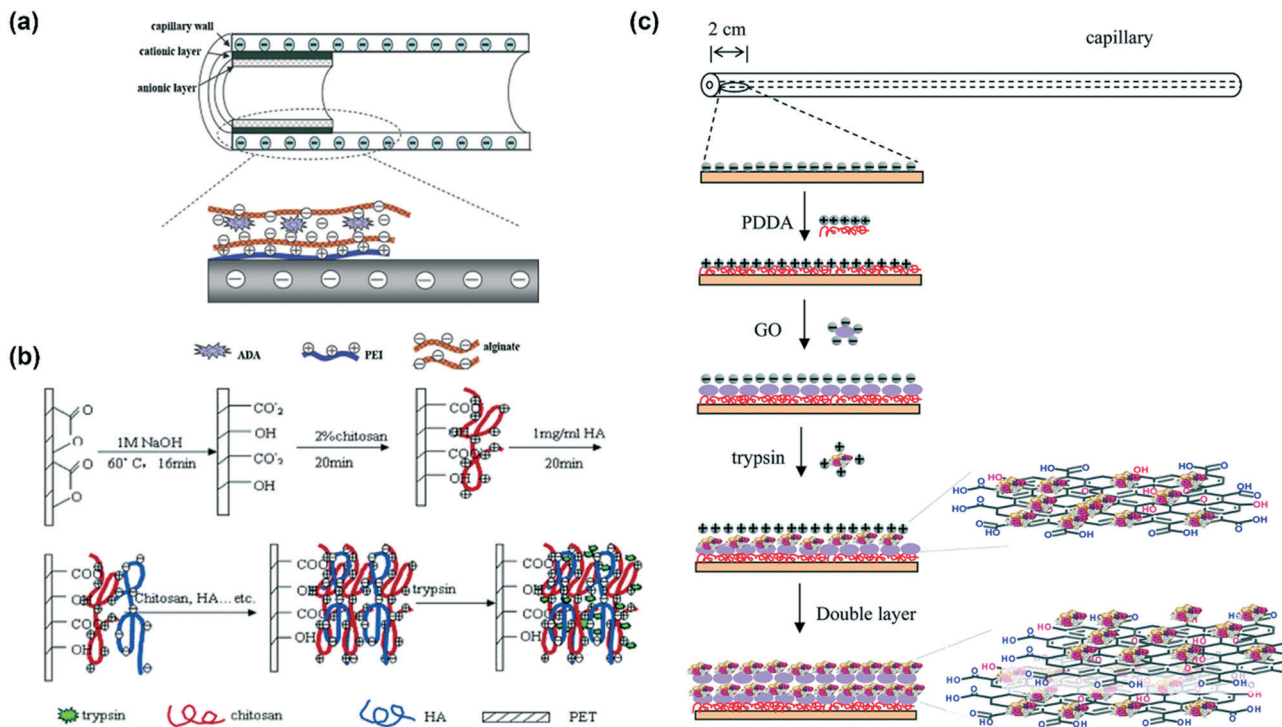


Fig. 9 Schematic representations of enzyme immobilization by ionic binding via different polycations and polyanions. (a) Adenosine deaminase (ADA) immobilization by PEI and alginate. Reproduced from ref. 122 with permission of Elsevier Ltd. (b) Trypsin immobilization by HA and chitosan. Reprinted with permission from ref. 34. Copyright 2006 American Chemical Society. (c) Trypsin immobilization by PDDA and negatively charged graphene oxide. Reproduced from ref. 69 with permission from The Royal Society of Chemistry.

4.1.3 Affinity binding. Affinity binding enables enzyme immobilization on the support *via* certain specific ligands, such as His-tag/metal binding, avidin/biotin binding, DNA-directed immobilization, and antigen/antibody binding. Therefore, this can ensure the higher loading amount and enzyme stability. Sometimes, more than one affinity binding method can be adopted into a single device to improve the binding efficiency and loading amount. In nonspecific enzyme immobilization methods, such as physical adsorption or covalent binding, the orientation of enzymes is difficult to control. Then, enzyme activities can deteriorate due to the blockage of active sites and conformational changes. However, in affinity binding, the orientation of enzymes can be effectively controlled to expose the active sites to the substrate, which helps to maintain the activities. Affinity binding can also be reversed by pH or temperature changes or certain special chemical treatments that can favor the reusability of microreactors. However, enzymes often need to be decorated with certain tags genetically or chemically to prepare for immobilization. This step makes affinity binding more complicated and costly as compared to the other methods.

A) His-tag/metal binding. Metal binding needs enzymes and supports to be bonded together by coordination with metals in between them. Generally, highly active, stable, and specific immobilized enzymes can be obtained by using this method.^{129–131} The enzyme-loading amount by this method is also usually higher than that required in other methods.^{111,130} In such cases, polyhistidine linkers can be

genetically tagged to the enzyme and then connected to nitrilotriacetic acid (NTA) attached on the support for enzyme immobilization. Recently, Kulsharova *et al.* immobilized transketolase (TK) in PMMA microfluidic devices by two methods using His-tag/nickel-NTA interactions: the 1-step-immobilization method (see Fig. 10a) and 3-step-immobilization method.¹¹² The device fabricated by the 1-step-immobilization method exhibited higher specific activity and reusability than that fabricated using the 3-step method. The 1-step method also required fewer chemicals and lesser time duration. Moreover, it was also demonstrated that His-tag/Ni binding had higher reversibility, facilitating the reuse of the microreactor.¹³²

However, this method also suffers from several intrinsic drawbacks. Sometimes, this method cannot be easily reproduced due to the formation of nonuniform adsorption sites and metal ion leakage.¹³³ Therefore, it is usually combined with covalent bonding or crosslinking to get a more stable formation of adsorption sites and chelation.

B) Avidin/biotin binding. Avidin/biotin binding is one of the most popular affinity binding techniques with high affinity and specificity. The interaction is regarded as the strongest noncovalent interaction¹³⁴ having the advantages of rapid fabrication and insensitivity to pH, temperature, proteolysis, and denaturing agents.^{83,113,135} Moreover, avidin or biotin can be easily modified by other chemicals, enabling more effective enzyme immobilization or certain other interesting functions.^{114,136}

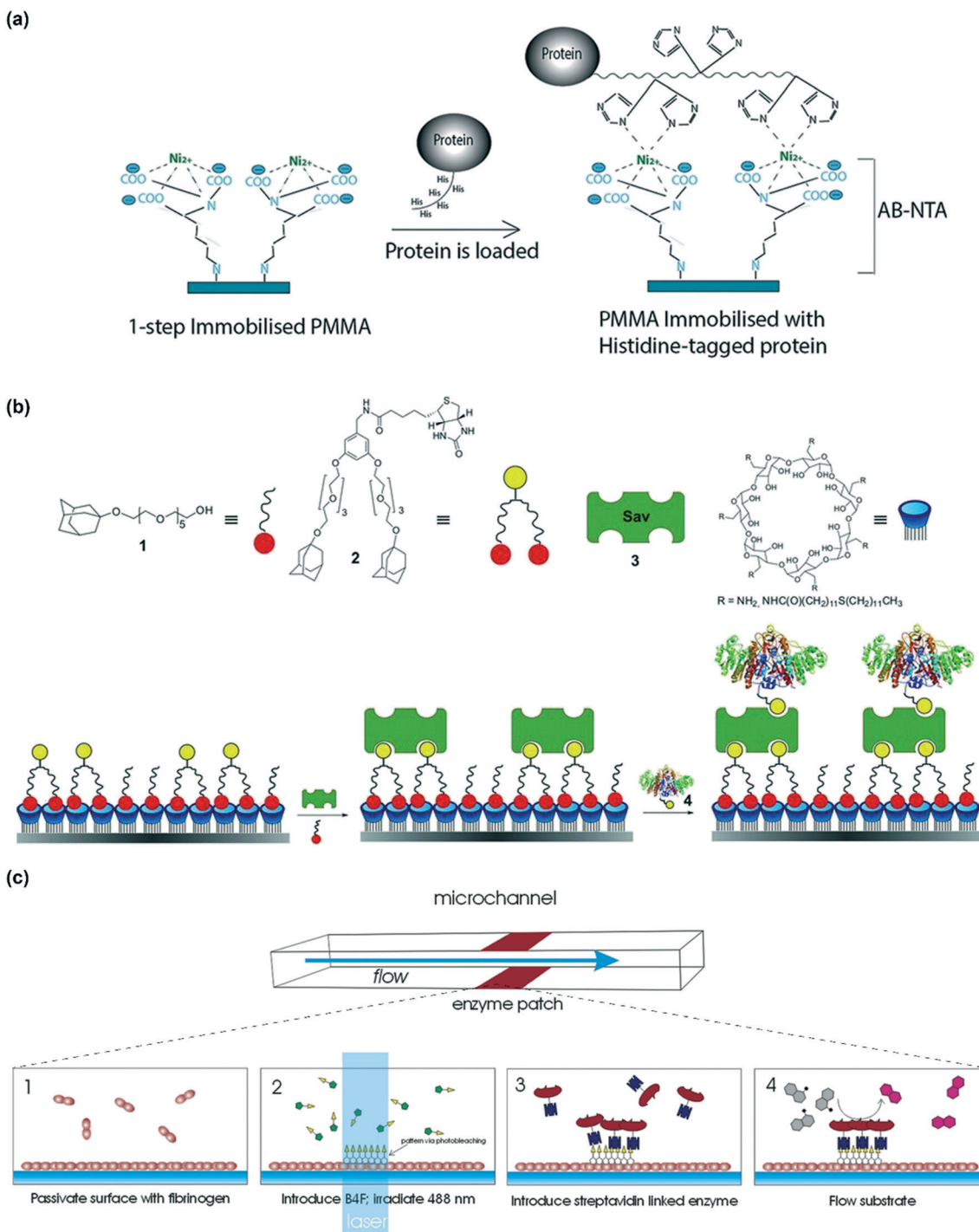


Fig. 10 Schematic representations of enzyme immobilization by His-tag/metal binding. (a) Diagram of enzyme immobilized by His-tag/Ni-NTA binding; reproduced from ref. 112 with permission from Elsevier Ltd. (b) Chemical structures of the building blocks and schematic of the stepwise assembly process. Ethylene-glycol-based mono-adamantyl linker (b1) for minimizing nonspecific protein adsorption, biotinylated bisadamantyl linker (b2) for the first assembly step, and streptavidin (b3) as the second assembly step. Biotinylated ALP (bt-ALP, 4) is immobilized onto these streptavidin-biotin surfaces. Reproduced with permission from ref. 136. Copyright 2004 American Chemical Society. (c) Schematic diagram of the photoimmobilization process. (Top) Enzyme patches are formed on the top and bottom of a microchannel using the following procedure: (c1) Passivation of the surface with a fibrinogen monolayer is followed by (c2) biotin-4-fluorescein surface attachment. This is accomplished by photobleaching with a 488 nm laser line. (c3) Next, the binding of streptavidin-linked enzymes that can be exploited to immobilize catalysts and (c4) to monitor the reaction processes on-chip. Reproduced from ref. 114 with permission from John Wiley & Sons, Inc.

González-Campo *et al.* developed a supramolecular platform with a combination of orthogonal supramolecular

interactions of the host (β -cyclodextrin)-guest (adamantane) and biotin-streptavidin interactions for the site-selective

immobilization of enzymes in a microchannel (Fig. 10b).¹³⁶ A microfluidic chip with a supramolecular platform was demonstrated to exhibit considerable reproducibility and reusability in enzyme reactions when calf intestine alkaline phosphatase (ALP) was used as the model enzyme. The site-selective immobilized ALP could also maintain comparable activity in other environments (free in solution or immobilization by other methods). Holden *et al.* also presented a study for the photoimmobilization of multiple enzymes in PDMS/glass microfluidic channels by site-specific immobilization (Fig. 10c).¹¹⁴ A biotin-linked dye solution was used to immobilize streptavidin-linked enzymes on select photo-patterning positions. The patterning of enzymes in a sequence inside microfluidic channels could be achieved by photobleaching instead of using valves.

C) DNA-directed immobilization. DNA-directed immobilization (DDI) is based on the Watson–Crick pairing mechanism between the single-strand DNA (ssDNA) attached on enzymes and complementary DNA (cDNA) attached to the supports. The attachment of ssDNA to enzymes can be usually accomplished by covalent binding or avidin/biotin binding.^{115,137,138} Generally, binding by DDI is more stable and robust than other methods, thereby yielding high immobilization efficiency and site-specificity. The DDI method is superior to others methods, mainly because of its ability of precisely controlling the relative positions of different enzymes,¹⁹ which is critical to cascaded enzyme reactions.

4.1.4 Covalent binding. Covalent binding is formed by the chemical reaction between the functional groups on the surface of a support and amino acid residues of the enzyme. The most commonly used covalent bonds are based on Schiff or carbodiimide chemistries, as shown in Fig. 11a.¹⁰ Since covalent binding always offers the strongest bond between

the enzyme and support, the enzyme usually exhibits high stability, promising reusability, and strong resistance to extreme environments. However, conformational change and activity reduction of the enzyme may occur after immobilization. Moreover, the orientation of the enzyme is harder to control as compared to that in specific immobilization, resulting in a decrease in the reaction rate. Nevertheless, blocking the active sites of the enzyme with a competitive inhibitor or substrate before immobilization may alleviate this problem.

Typically, only one layer of covalently immobilized enzyme can be formed on the surface of the support. Then, the loading amount can become very limited. Therefore, a crosslinker may be used to form enzyme polymerization to facilitate this increase. Lloret *et al.* prepared a laccase-immobilized microreactor by the formation of an enzyme-polymer membrane on the inner wall of the microtubes (Fig. 11b–d).¹³⁹ This membrane was formed by the crosslinking polymerization reaction between laccase and crosslinkers (paraformaldehyde and glutaraldehyde). The microreactor with crosslinked laccase not only exhibited important biotransformation efficiency when compared with conventional bioreactors, but also exhibited excellent pH, temperature, inactivating agent, storage, and long-term stabilities.

4.2 Encapsulation

The encapsulation of an enzyme is defined as the enzyme entrapped inside a small space that allows the substrates and products to pass through but retains the enzyme. It mainly includes matrix entrapment and membrane encapsulation, as shown in Fig. 8. For matrix entrapment, the enzymes are entrapped into a matrix, which is usually formed by polymers

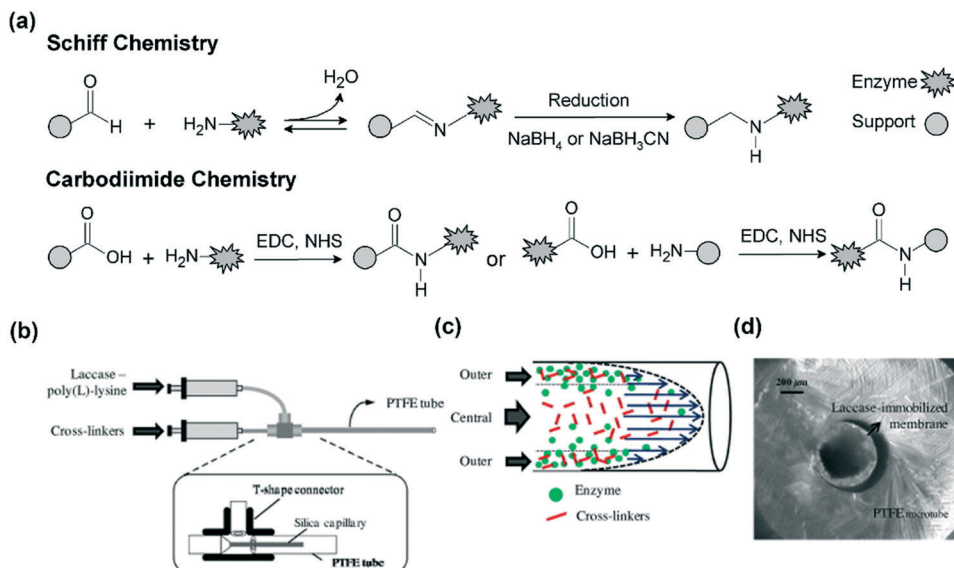


Fig. 11 Covalent binding for enzyme immobilization. (a) Commonly used covalent bonds: mechanisms of Schiff chemistry and carbodiimide chemistry; reproduced from ref. 10 with permission from Elsevier Ltd. (b) Preparation of laccase-immobilized membrane on the inner wall of a PTFE microtube. (c) Parabolic velocity profile characteristic of the laminar flow inside a microtube and (d) confocal acquisition of the sectional view of a laccase-immobilized microreactor (dry state). These three figures were reproduced from ref. 139 with permission from Elsevier Ltd.

(like alginate^{122,123} and PEG hydrogels^{120,140,141}) or other inorganic materials (like titania¹¹⁸ and silica sol-gels^{97,117,142}). When a semipermeable membrane, like a hollow fiber¹⁴³ or microencapsulate,¹⁴⁴ is used to encapsulate the enzymes, it is classified as membrane encapsulation. When compared with physical adsorption, the entrapment method is more stable and can immobilize a larger amount of enzyme. In addition, this entrapment does not need the chemical modification of the enzyme, which not only saves time but also avoids any conformational changes in the enzyme. However, the slower diffusion of the substrate to the

enzyme in this case may severely restrict biocatalytic production. Further, there are possibilities of enzyme leakage and enzyme contamination by the matrix. Moreover, the microenvironments of the matrix are difficult to control, which may lead to a reduction in the enzyme activity and stability. However, there is a great opportunity to reduce the impact of these problems by carefully choosing the polymer materials with proper modification and by adjusting the pore size or capsule size. Moreover, capsules can imitate the multicompartment structures of cellular architectures to encapsulate enzymes in a controllable number, type, and

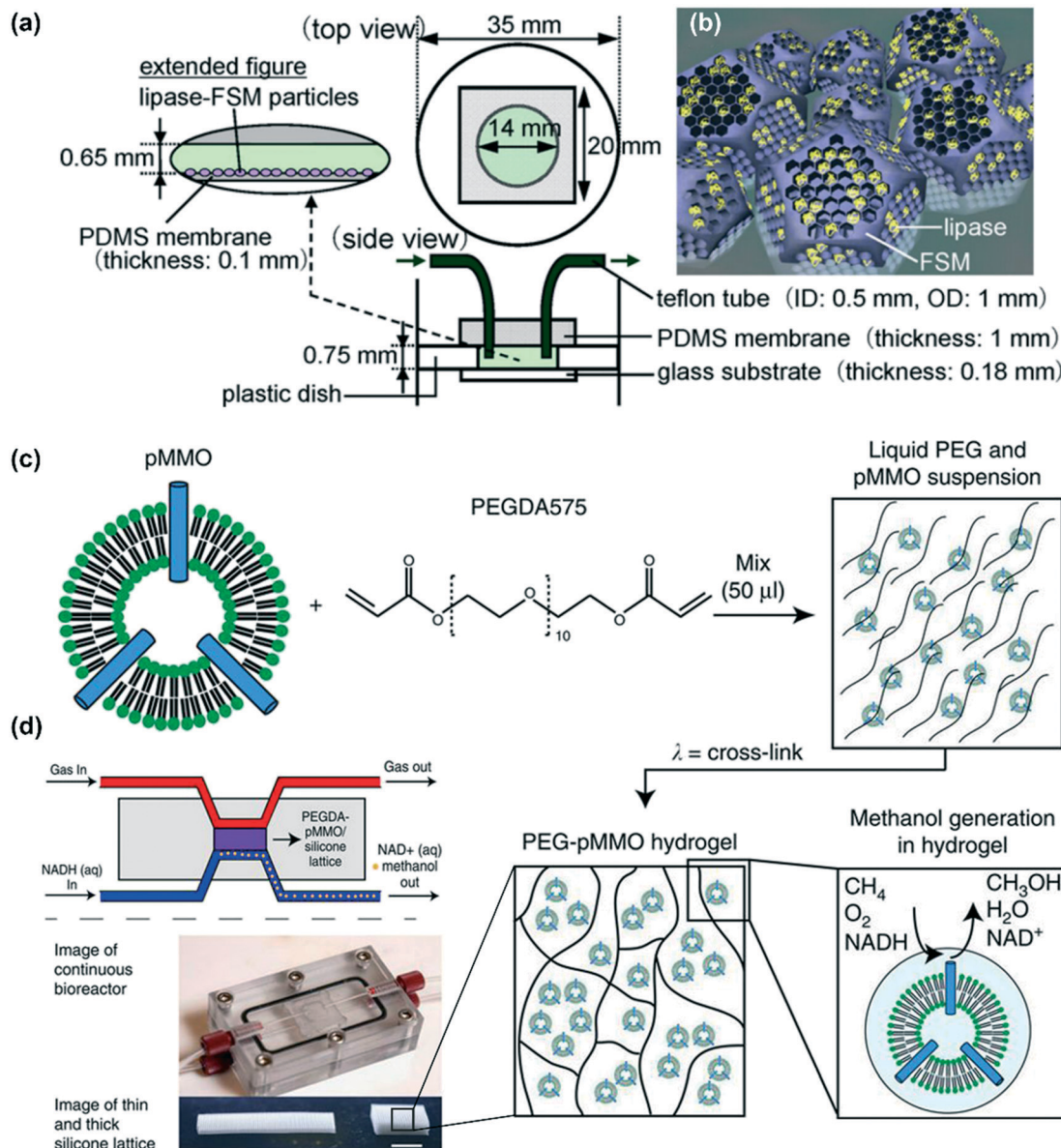


Fig. 12 Examples of enzyme immobilization by encapsulation. (a) Schematic illustrations of the microreactor with immobilized lipase–nanoporous material (FSM) composite particles; (b) lipase molecules encapsulated in the FSM pores; these two figures were reproduced from ref. 119 with permission from Elsevier Ltd. (c) Schematic of PEG-pMMO hydrogel fabrication. Membrane-bound pMMO is mixed with PEGDA 575 and photoinitiator and exposed to ultraviolet light to crosslink the material. (d) Schematic and image of the flow-through bioreactor and two (thin and thick) silicone lattice structures used to support the PEG-pMMO hydrogel membrane (scale bar: 1 cm); these two figures were reproduced from ref. 140 with permission from Springer Nature.

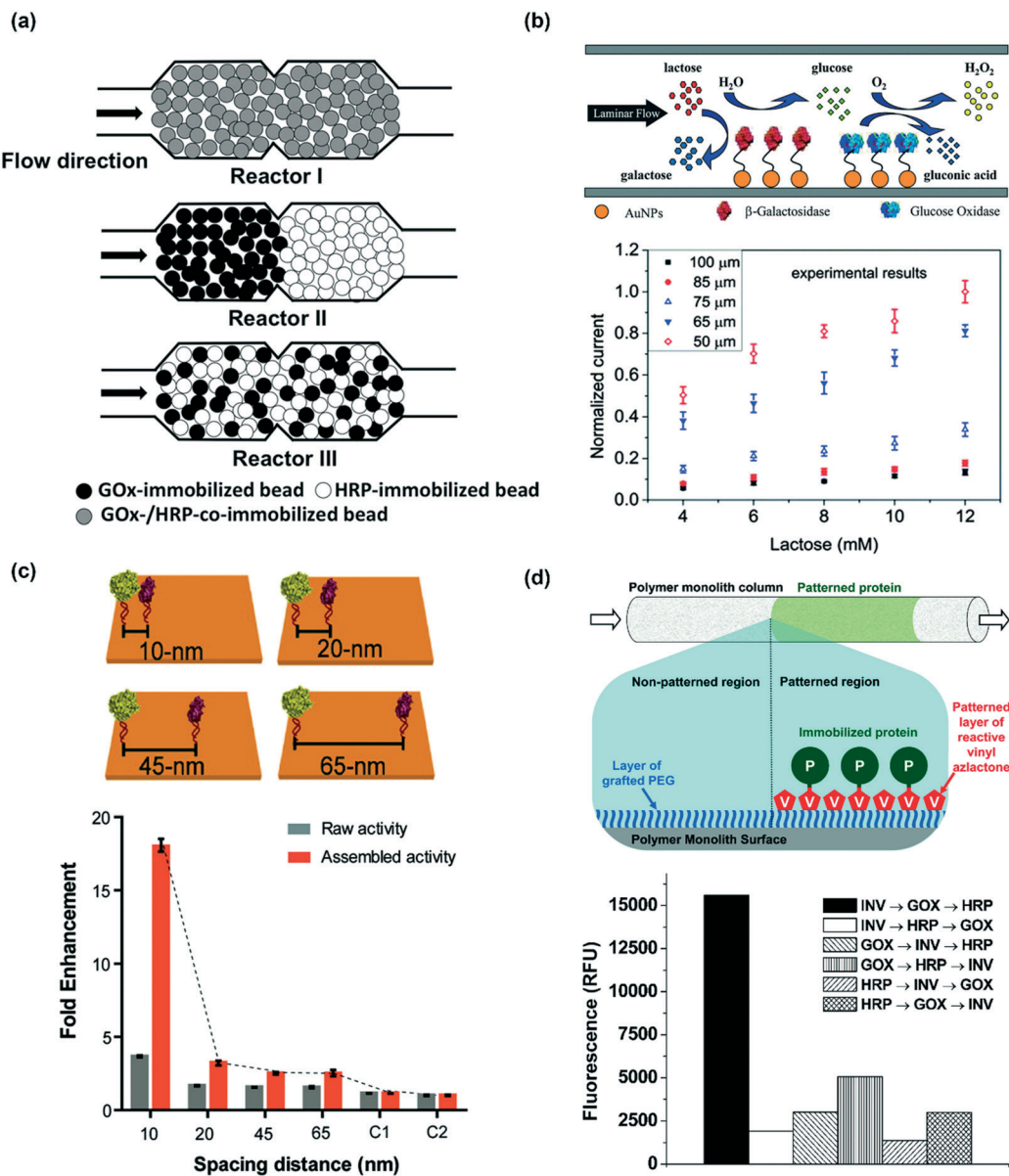


Fig. 13 Examples of enzyme immobilization in multienzyme systems. (a) Diagrams of three different configurations of microfluidic reactors. In Reactor I, GOx and HRP were coimmobilized on a single set of beads. In Reactor II, GOx- and HRP-immobilized beads were sequentially loaded. In Reactor III, the two beads were mixed in the reactor. Reprinted with permission from ref. 156. Copyright 2014 Japan Society for Analytical Chemistry. (b) Schematic of the enzyme cascade reaction confined in a microchannel. Here, β-galactosidase and glucose oxidase were assembled on gold films within controllable distances (up). Graph of the normalized response currents of H₂O₂ as a function of the concentration of lactose with different gap distances in the experiment (down). Reproduced from ref. 116 with permission from the PCCP Owner Societies. (c) Rectangular DNA origami tiles with assembled GOx (yellow) and HRP (purple) pairs spaced from 10 to 65 nm (up). Enhancement of the activity of the enzyme pairs on DNA nanostructures as compared to those of the free enzyme in a solution (down). The largest enhancement factor was observed when the interenzyme distance was decreased to 10 nm, as analyzed with D-glucose, ABTS₂-[2,2'-azinobis(3-ethylbenzothiazoline-6-sulfonate)], and O₂ as substrates at pH 7.2. C₁ and C₂ refer to the tiles without nucleic acid and free enzymes, respectively. Reprinted with permission from ref. 158. Copyright 2012 American Chemical Society. (d) Schematic representation of the microfluidic setup used for performing sequential synthesis with a three-enzyme system: invertase (INV), GOX, and HRP. Enzymes were immobilized on the surface of a polymer monolith in patterned regions within a microfluidic channel. Polyethylene glycol (PEG) was grafted onto the surface of the polymer monolith to prevent nonspecific protein adsorption. Vinyl azlactone is photopatterned onto the PEG surface, which activates the surface for protein immobilization (up). Product fluorescence intensities measured with each possible arrangement of the three enzymes are shown in the figure legend (down). The substrate solution consisted of 10 mg mL⁻¹ sucrose, 100 μmol L⁻¹ Amplex Red (10-acetyl-3,7-dihydroxyphenoxazine), and 1.0% (v/v) dimethyl sulfoxide (DMSO) in 50 mmol L⁻¹ phosphate buffer, pH 7.50; pure oxygen was bubbled through this solution for 15 min prior to use. The flow rate was 0.10 μL min⁻¹. Reprinted with permission from ref. 95. Copyright 2007 American Chemical Society.

spatial arrangement, thereby maintaining or even enhancing the overall catalytic activity.^{145,146}

Mizukami developed a microreactor containing lipases encapsulated in folded-sheet mesoporous (FSM) silicas with two different pore diameters (Fig. 12a and b).¹¹⁹ FSM with larger diameters (~7 nm) (FSM7) indicated a higher enzyme-loading amount than FSM with a smaller diameter (~4 nm) (FSM4). The two types of lipase FSM silicas were loaded in the microreactors for the hydrolysis of a triglyceride; both of them exhibited higher enzyme activity than that by the batch reaction. The results also revealed that the enzyme activity in lipase-FSM7 was slightly higher than that in lipase-FSM4. This may be attributed to the larger pore size of FSM7, which facilitates the access of the substrate to the encapsulated enzyme. Blanchette *et al.* entrapped the active particulate methane monooxygenase (pMMO) and associated lipids in a PEG-based hydrogel (Fig. 12c).¹⁴⁰ The hybrid materials were then suspended between the gas and liquid reservoirs in a flow-through reactor (Fig. 12d). With this configuration, a methane/air gas mixture and NADH could be constantly introduced into the reactor while continuously removing and collecting methanol in a buffer. The native conformation and physiological activity of pMMO are completely retained by this encapsulation method. In addition, this strategy enables the reuse and continuous use of pMMO. Moreover, this method allows the facile fabrication of immobilization structures in 3D structures from the micro to millimeter scales, which guarantees the higher loading of pMMO when compared with that obtainable through surface immobilization.

5. Multienzyme systems

Most natural biocatalytic reactions are catalyzed by more than one enzyme. Tremendous efforts have been devoted toward immobilizing multiple enzymes in one microfluidic reactor to artificially construct various biocatalytic reactions observed in nature.^{76,95,116,137,141,147–149} The methods for multienzyme immobilization are based on those involving single-enzyme immobilization. However, careful consideration should be made to maintain the activities and catalytic efficiencies of all the enzymes according to the structures and optimal environments of the different enzymes. One major issue for multienzyme immobilization is the control of their relative spatial positions in a single reactor, although it is much easier for microfluidic reactors as compared to that for batch reactors. The well-controlled spatial positions would probably promote an increase in the reaction rate and catalytic efficiency. The unwanted side reactions and accumulation of inhibitors or reactive intermediates may also be avoided.^{150–154}

Multiple enzymes can be immobilized in one pot,^{141,148} sequentially,^{115,116,137} or LBL assembly.¹⁵⁵ Heo *et al.* packed GOx- and HRP-bearing microbeads into microfluidic reactors with different spatial distances, as shown in Fig. 13a.¹⁵⁶ Reactor I packed the microbeads coimmobilizing both GOx

and HRP. Reactor II had GOx-immobilized microbeads packed in front of the HRP-immobilized microbeads. In Reactor III, GOx- and HRP-immobilized microbeads were mixed and packed. It was demonstrated that better overall reaction efficiency could be obtained in Reactor I than those obtainable with the other two reactors. The increased efficiency due to the decreased enzyme distance can be attributed to the reduced diffusional loss of the intermediate product (hydrogen peroxide, H₂O₂) and the prevention of inhibitor accumulation. Another work presented by Wu *et al.* investigated the distance for multienzyme immobilization in micrometers and arrived at a similar result.¹¹⁶ Further, β-galactosidase and glucose oxidase were immobilized on two separate gold films patterned within a single microfluidic channel, as shown in Fig. 13b. The highest conversion efficiency of the cascaded reaction was obtained when the two enzymes were within minimum distance (50 μm). Even though the spatial positions of the enzymes are easy to control by separating the microchannels into multiple areas, they are still not very close to each other like that in the case of natural cascaded systems.¹⁵⁷ Therefore, researchers have been paying attention to a combination of microfluidic reactors and DDI, wherein more precise spatial control can be obtained toward reaction efficiency enhancement. It has been demonstrated that when the GOx and HRP enzymes were immobilized *via* DNA origami tiles at a distance of 10 nm from each other, an increase of more than 15-fold in the overall cascade activity was observed as compared to that when using free enzymes, as shown in Fig. 13c.¹⁵⁸ The reason for this activity increase was suggested to be the efficient transport of the reaction intermediate (H₂O₂) between the two enzymes.

The sequential order is also very important for the overall reaction efficiency in multienzyme systems. As shown in Fig. 13d, three enzymes (INV, GOx, and HRP) were spatially immobilized by a photopatterning method on porous polymer monoliths within microfluidic devices.⁹⁵ The three-enzyme system was used to perform a sequential reaction with sucrose hydrolyzed to glucose and fructose by INV in the first step. Then, GOx would oxidize glucose to gluconolactone and H₂O₂, which was subsequent to the oxidation by HRP to Amplex Red. Among all the six possible arrangements of the three enzymes, the correct sequential order of the catalyst (INV-GOx-HRP) resulted in the highest resorufin fluorescence by more than three folds. This demonstrates that the correct enzyme order is critical for the reaction efficiency in multienzyme-immobilized microfluidic systems.

6. Scalability of microfluidic reactors

The application of microfluidic reactors to biocatalysis exhibits several inherent benefits, such as rapid heat transfer, precise reaction control, and capability for continuous and integrated operation. Microfluidic reactors are also advantageous because of their robust structures, capacity,

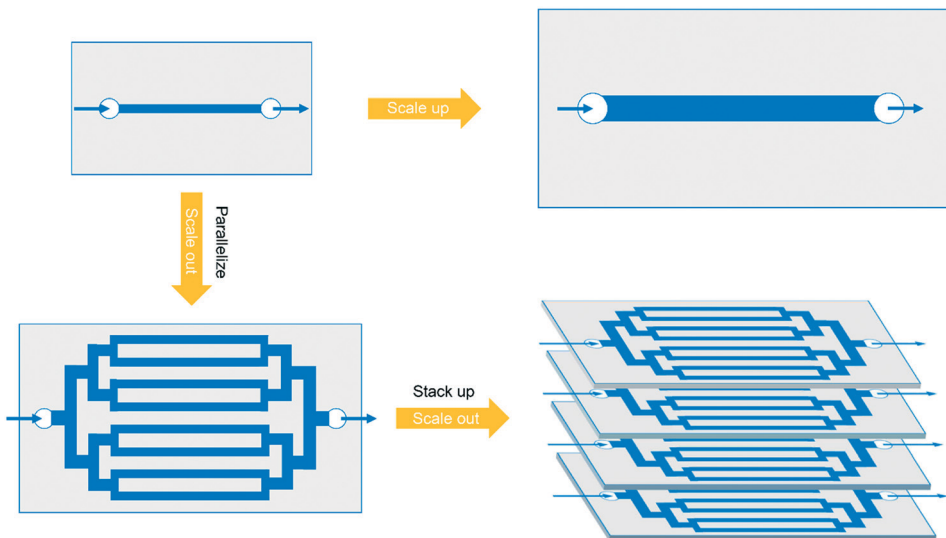


Fig. 14 Illustration of the concept of scaling the microreactors both upward and outward. Scaling up means increasing the characteristic dimensions of the channel. Scaling out refers to the fact that parallel reactor systems or multiple microreactors are stacked up.

and ease of scalability for mass production.^{17,159} These are particularly attractive toward the synthesis of petrochemicals, active pharmaceutical ingredients, or value-added materials in the industry. Generally, two methods for scaling microfluidic reactors have been widely discussed: scaling up (increasing the characteristic dimensions of the channel) and scaling out (using parallel reactor systems or stacking up multiple microreactors), as shown in Fig. 14.

Many reviews have comprehensively discussed the microreactor design and scale-up concept.^{20,160–162} The principle for scaling up a single-channel reactor is presented as the relationship between its characteristic dimension and the mixing and heat transfer characteristics. Some studies also use mathematical models comprising the reaction kinetics and flow dynamics to optimize the reaction conditions and reactor designs for scaling up.^{163–166} With regard to scaling out, it has its own advantages over scaling up in maintaining the reactions performed in each reactors to the same intensity at any level.^{167,168} Generally, scaling out is practicable by designing a multiple-channel reactor with only one pump and heating apparatus.¹⁶⁹ Uniform flow distribution as well as the same residence time in all the microchannels should be ensured when designing the manifold structures. Amador studied an analytical model based on the electrical resistance networks for two manifold structures to describe the flow in each microchannel.¹⁷⁰ Based on this model, the design and fabrication of scale-out microreactors applied to different operation conditions are feasible.

Recently, Bajić *et al.* conducted a scale-up study on a two-plate miniaturized packed-bed reactor (MPBR) in which LentiKats® (lens-shaped PVA particles) encapsulated with ω -transaminase (ω -TA) were uniformly or randomly packed (as shown in Fig. 15a).¹⁴⁴ MPBRs were used for the synthesis of acetophenone (ACP) and L-alanine (L-ALA) from (S)- α -

methylbenzylamine ((S)- α -MBA) and sodium pyruvate (PYR). The productivity was evaluated by increasing the capacity of the reactor from microliter to milliliter by adjusting the length, width, and depth of the channel. Fig. 15b shows the three representative reactors by scaling up in terms of width. The results revealed that increasing the length and width would increase the productivity; however, increasing the depth would reduce it. Here, the flow distribution that encourages the accessibility of the substrates to the immobilized enzyme is the key for increasing the productivity with an increase in the reactor size. This study provided a simple but efficient guide for scaling up. However, for commercial-scale production, a combination of scaling up and scaling out may be the best option.¹⁶⁹ In addition, for a continuous reaction, the production amount can be increased by simply increasing the operation time without changing the reaction conditions. Therefore, large-scale production can be achieved in a simple, green, and cost-effective way.

As one of the earliest applications of immobilized enzyme for use in biocatalysis in a continuous flow, Liu *et al.* reported the continuous production of uridine diphosphate galactose (UDP-Gal) by circulating galactose (Gal), uracil monophosphate (UMP), and polyphosphate (polyP) through a column packed with seven enzyme-immobilized agarose beads, as shown in Fig. 16a.¹⁷¹ The enzymes were immobilized by histidine tags on nickel agarose beads. Small-scale reactions on mini Pasteur pipette columns were initially carried out to optimize the reaction conditions. Then, a packed-bed column was scaled up to the gram scale to conform to practical biosynthesis. When compared with the solution reaction, the on-column reaction results in higher product yields in a long-time reaction (50% of the UMP converted into UDP-Gal in 48 h) when compared with the solution reactions, which can be attributed to the

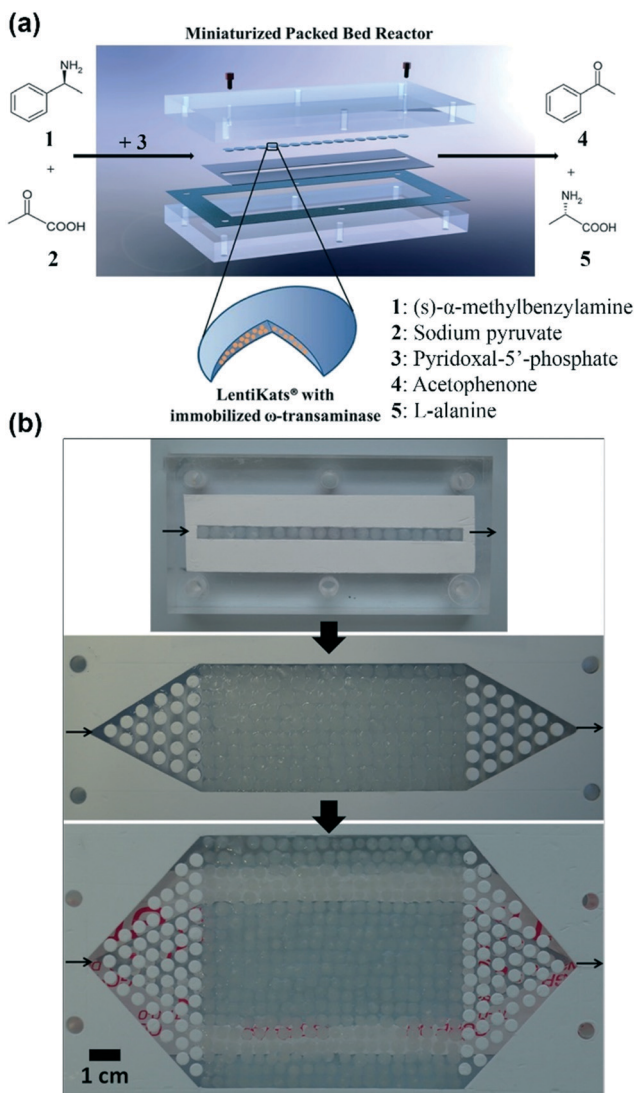


Fig. 15 (a) Diagram of a miniaturized packed-bed reactor (MPBR) packing LentiKats® with immobilized ω -transaminase for performing continuous enzyme process. (b) MPBRs exhibiting the scale-up situation with regard to channel width. MPBRs from up to down: ~4 mm-wide rectangular channel, hexagonal channel (rectangular part is ~40 mm wide) with a triangular inlet and outlet parts containing pillars, and hexagonal channel (rectangular part is ~80 mm wide) with a triangular inlet and outlet parts containing pillars. Reproduced from ref. 144 with the permission of Elsevier Ltd.

reusability and stability of the immobilized enzyme (Fig. 16b). This continuous synthesis of UDP-Gal can help in alleviating difficulties in the production of sugar nucleotides, which is important for the synthesis of pharmaceutically valuable oligosaccharides. Orsat *et al.* reported a continuous acylation process to produce monoacylated Vitamin A precursors from 1,6-diol by immobilized lipase Chirazyme L2-C2 (lipase B from *Candida antarctica*).¹⁷² A laboratory-scale fixed-bed reactor was initially utilized to investigate the optimal reaction conditions with >99% yield and >97% selectivity at a yield of 49 g day⁻¹. Then, a kilogram-scale reactor was accordingly prepared at a throughput of 1.6 kg

day⁻¹ over 100 days. The production of Vitamin A precursors is environment-friendly, robust, and sustainable as a result of the recyclable chemicals. Some recent studies have also demonstrated the successful scaling up of μ -IMERs for biocatalytic synthesis.^{173–175}

7. Summary and outlook

Biocatalytic reactions play an important role in biochemistry because of their environmental-friendliness, high efficiency, and strong selectivity. However, the most popular biocatalyst—enzymes—often fail to retain the activity and stability in practical applications. Here, μ -IMERs for continuous biocatalysis have drawn on the benefits of both microfluidic reactors and enzyme immobilization techniques for effecting highly efficient, stable, reproducible, and continuous biocatalytic reactions in both laboratory and industry. In this review, different factors that affect the production efficiency, stability, and reusability in μ -IMERs have been summarized following a top-down strategy.

From the macroscopic aspect, the materials used for microfluidic reactors should be temperature- and chemically stable, biocompatible with enzymes, and easy to fabricate. Among all the organic and inorganic materials (glass, silicon, PDMS, PMMA, PC, paper, *etc.*), PDMS is the most popular. It not only meets all the requirements mentioned above, but also has the advantages of optical transparency, promising flexibility, and easy surface modification. Once the fabrication material is chosen, the configuration of microfluidic reactors should also be effectively designed to make full use of the space for enzyme loading and substrate access. Fabrication technologies of microfluidic reactors should also be effectively chosen according to the materials and configurations.

From the microscopic aspect, the internal structures of microfluidic reactors should provide a large specific area for enzyme loading and a short diffusion path to facilitate the affinity of substrate to enzyme. There are three main types of microfluidic channels: wall-coated, packed-bed, and monolithic. Generally, wall-coated channels have the least impact of diffusion resistance on enzyme activity. However, they usually possess a lower specific area and longer diffusion path. Nevertheless, packed-bed channels have the shortcomings of immense pressure drops. It is also difficult to control fluids and heat transfer inside packed-bed channels. For monolithic channels, certain problems such as nonuniform permeability, poor reproducibility, and time-consuming fabrication may limit their applications. Overall, each of them has its own strengths and weaknesses, and it is difficult to say which one is the best. The design of internal structures should balance every aspect and take into account the used enzyme immobilization technique.

From the nanoscopic aspect, the choice of enzyme immobilization technique is a major factor that affects the overall biocatalytic efficiency of μ -IMERs. For most noncovalent binding methods, they have the advantages of

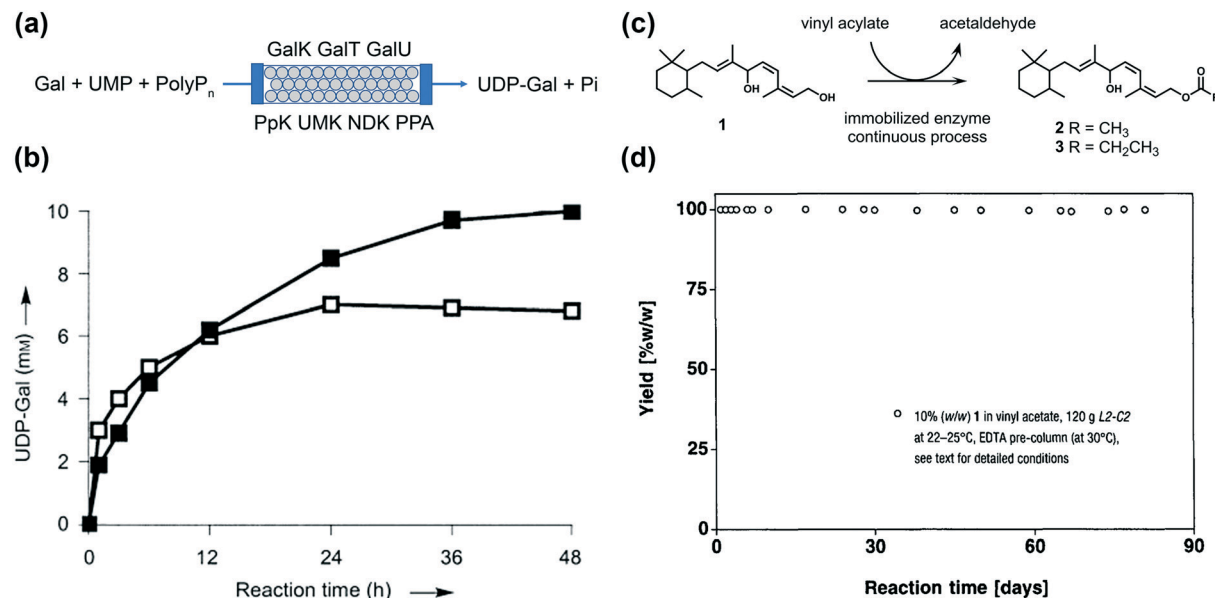


Fig. 16 (a) Biosynthesis of UDP-Gal in a continuous packed-bed column with seven immobilized enzymes. The starting materials are Gal, UMP, and polyP. Seven enzymes were used for the catalysis: galactokinase (GalK, EC 2.7.1.6), galactose-1-phosphate uridylyltransferase (GalT, EC 2.7.7.10), UDP-glucose pyrophosphorylase (GalU, EC 2.7.7.9), polyphosphate kinase (PpK, EC 2.7.4.1), uridine monophosphate kinase (UMK, EC 2.7.4.14), nucleotide diphosphate kinase (NDK, EC 2.7.4.6), and pyrophosphatase (PPA, EC 3.6.1.1). UDP-Gal and two phosphates (Pi) were formed in the end. (b) Time course of UDP-Gal production. The reaction on the super-bead column (200 mL, filled squares) was performed with UMP and Gal (20 mM each), polyP (2% (w/v)), ATP, and glucose-1-phosphate (2 mM each). About 50% UMP was converted into UDP-Gal within 48 h. Reaction in the solution with the purified enzymes (50 mL, open squares) used the same reaction composition. About 35% UMP was converted in 24 h. Reproduced from ref. 171 with the permission of John Wiley and Sons. (c) Principle of the lipase Chirazyme L2-C2-catalyzed acylation of 1,6-diol (1). (d) Continuous miniplant production of 2 catalyzed by L2-C2 at 22–25 °C in the presence of 10% (w/w) of 1 in vinyl acetate. The throughput was readjusted after 74 d. Reproduced from ref. 172 with the permission of CHIMIA.

simple fabrication, mild immobilization conditions, low chance of conformational change, and promising reversibility. However, the bonds are generally weak and dependent on pH or ionic strength. For performance improvement, covalent binding is usually employed to provide stronger and more stable interactions for the enzyme and support. However, enzyme conformation can be changed by using covalent binding, which—to some extent—may reduce the activity. In addition, these nonspecific methods cannot control the orientation of enzymes, which may cause the blockage of active sites by the support. This problem may be resolved by site-specific affinity binding, which can precisely control the orientation of enzymes and expose their active center to the substrate. Site-specific binding also enables the fine positioning of different enzymes within confined spaces, which is noted to play a key role in multienzyme systems. With regard to encapsulation, it offers a three-dimensional matrix for enzyme immobilization. Then, the enzyme-loading amount would be relatively larger than that required by surface binding methods. Nevertheless, there are certain drawbacks such as slow diffusion of the substrate to the enzyme, enzyme leakage, or enzyme contamination by encapsulation materials. On account of these, there is no perfect immobilization method. More than one strategy is often combined to optimize the activity, stability, and reusability of enzymes.

μ-IMERs for continuous biocatalysis can be expanded from laboratory to industry for large-scale production by scaling up and scaling out if the reaction kinetics and flow dynamics are carefully considered. However, difficulties persist for wider applications due to the numerous and complex issues involved. The challenges also include simplifying the fabrication process, increasing activity, and reducing cost. Some new nanomaterials or nanostructures with high SAV ratios have already been developed as enzyme immobilization carriers, such as molybdenum disulfide,^{176,177} halloysite nanotubes,^{178–180} metal-organic frameworks,^{181–183} and so on. However, there is still a lack of research in the integration of enzyme-loaded new nanomaterials with microfluidic reactors for use in biocatalysis. Further, it is necessary to increase the type of enzymes used for μ-IMERs and not limited to common model enzymes such as trypsin, lipase, GOx, or HRP. In the future, μ-IMERs with a new configuration design and new enzyme immobilization method could be applied to a variety of biocatalysis situations in both experimental research and industrial production.

Conflicts of interest

There are no conflicts of interest to declare.

Acknowledgements

This work is supported by National Science Foundation of China (no. 61377068) and Research Grants Council (RGC) of Hong Kong (N_PolyU505/13, 152184/15E, 152127/17E, 152126/18E and 152219/19E). The authors would like to thank The Hong Kong Polytechnic University for the grants G-YBPR, 4-BCAL, 1-ZE14, 1-ZE27 and 1-ZVGH. The Science and Technology Development Fund, Macau SAR (File No. FDCT 0053/2019/A1, and AMSV SKL Fund) and University of Macau (MYRG2018-00114-AMSV) is also appreciated.

References

- L. Tamborini, P. Fernandes, F. Paradisi and F. Molinari, *Trends Biotechnol.*, 2017, **36**, 73–88.
- A. Schmid, J. Dordick, B. Hauer, A. Kiener, M. Wubbolt and B. Witholt, *Nature*, 2001, **409**, 258–268.
- X. Zhao, F. Qi, C. Yuan, W. Du and D. Liu, *Renewable Sustainable Energy Rev.*, 2015, **44**, 182–197.
- D.-M. Liu, J. Chen and Y.-P. Shi, *TrAC, Trends Anal. Chem.*, 2018, **102**, 332–342.
- C. Mateo, J. M. Palomo, G. Fernandez-Lorente, J. M. Guisan and R. Fernandez-Lafuente, *Enzyme Microb. Technol.*, 2007, **40**, 1451–1463.
- S. Cantone, V. Ferrario, L. Corici, C. Ebert, D. Fattor, P. Spizzo and L. Gardossi, *Chem. Soc. Rev.*, 2013, **42**, 6262–6276.
- A. Liese and L. Hilterhaus, *Chem. Soc. Rev.*, 2013, **42**, 6236–6249.
- N. R. Mohamad, N. H. C. Marzuki, N. A. Buang, F. Huyop and R. A. Wahab, *Biotechnol. Biotechnol. Equip.*, 2015, **29**, 205–220.
- R. A. Sheldon and S. van Pelt, *Chem. Soc. Rev.*, 2013, **42**, 6223–6235.
- K. Meller, M. Szumski and B. Buszewski, *Sens. Actuators, B*, 2016, **224**, 84–106.
- J. Britton, S. Majumdar and G. A. Weiss, *Chem. Soc. Rev.*, 2018, **47**, 5891–5918.
- M. P. van der Helm, P. Bracco, H. Busch, K. Szymańska, A. B. Jarzębski and U. Hanefeld, *Catal. Sci. Technol.*, 2019, **9**, 1189–1200.
- V. Hessel, S. Hardt and H. Löwe, *A Multi-Faceted, Hierarchic Analysis of Chemical Micro Process Technology: Sections 1.1–1.5*, Wiley Online Library, 2004.
- E. Wolfgang, H. Volker and L. Holger, *Microreactors: New Technology for Modern Chemistry*, Wiley/VCH, Weinheim, 2000, pp. 41–84.
- N. Wang, X. Zhang, Y. Wang, W. Yu and H. L. Chan, *Lab Chip*, 2014, **14**, 1074–1082.
- Y. Liu and X. Jiang, *Lab Chip*, 2017, **17**, 3960–3978.
- K. S. Elvira, X. C. I. Solvas and R. C. Wootton, *Nat. Chem.*, 2013, **5**, 905.
- M. B. Plutschack, B. U. Pieber, K. Gilmore and P. H. Seeberger, *Chem. Rev.*, 2017, **117**, 11796–11893.
- F. Jia, B. Narasimhan and S. Mallapragada, *Biotechnol. Bioeng.*, 2014, **111**, 209–222.
- J. Zhang, K. Wang, A. R. Teixeira, K. F. Jensen and G. Luo, *Annu. Rev. Chem. Biomol. Eng.*, 2017, **8**, 285–305.
- R. Porta, M. Benaglia and A. Puglisi, *Org. Process Res. Dev.*, 2015, **20**, 2–25.
- M. Planchestainer, M. L. Contente, J. Cassidy, F. Molinari, L. Tamborini and F. Paradisi, *Green Chem.*, 2017, **19**, 372–375.
- M. P. Thompson, I. Peñafiel, S. C. Cosgrove and N. J. Turner, *Org. Process Res. Dev.*, 2018, **23**, 9–18.
- E. Laurenti and A. dos Santos Vianna Jr, *Biocatalysis*, 2016, **1**, 148–165.
- S. R. Forrest, B. B. Elmore and J. D. Palmer, *Catal. Today*, 2007, **120**, 30–34.
- P. Abgrall and A. Gue, *J. Micromech. Microeng.*, 2007, **17**, R15.
- D. Kim and A. E. Herr, *Biomicrofluidics*, 2013, **7**, 041501.
- K. F. Lei, in *Microfluidics in Detection Science*, 2014, pp. 1–28.
- L. M. C. Ferreira, E. T. Da Costa, C. L. Do Lago and L. Angnes, *Biosens. Bioelectron.*, 2013, **47**, 539–544.
- M. R. F. Cerqueira, D. Grasseschi, R. C. Matos and L. Angnes, *Talanta*, 2014, **126**, 20–26.
- M. R. F. Cerqueira, M. S. F. Santos, R. C. Matos, I. G. R. Gutz and L. Angnes, *Microchem. J.*, 2015, **118**, 231–237.
- X. Hu, Y. Dong, Q. He, H. Chen and Z. Zhu, *J. Chromatogr., B*, 2015, **990**, 96–103.
- D. Ogończyk, P. Jankowski and P. Garstecki, *Lab Chip*, 2012, **12**, 2743–2748.
- Y. Liu, H. Lu, W. Zhong, P. Song, J. Kong, P. Yang, H. H. Girault and B. Liu, *Anal. Chem.*, 2006, **78**, 801–808.
- Y. Bi, H. Zhou, H. Jia and P. Wei, *RSC Adv.*, 2017, **7**, 12283–12291.
- T. Honda, M. Miyazaki, H. Nakamura and H. Maeda, *Adv. Synth. Catal.*, 2006, **348**, 2163–2171.
- H. Becker and C. Gärtner, *Electrophoresis*, 2000, **21**, 12–26.
- H. Becker and L. E. Locascio, *Talanta*, 2002, **56**, 267–287.
- A. Alrifaiy, O. A. Lindahl and K. Ramser, *Polymer*, 2012, **4**, 1349–1398.
- E. Roy, A. Pallandre, B. Zribi, M. C. Horny, F. D. Delapierre, A. Cattoni, J. Gamby and A. M. Haghiri-Gosnet, in *Advances in Microfluidics-New Applications in Biology, Energy, and Materials Sciences*, InTech, 2016.
- J. P. McMullen and K. F. Jensen, *Annu. Rev. Anal. Chem.*, 2010, **3**, 19–42.
- P. Lisowski and P. K. Zarzycki, *Chromatographia*, 2013, **76**, 1201–1214.
- F. Figueredo, P. T. Garcia, E. Cortón and W. K. Coltro, *ACS Appl. Mater. Interfaces*, 2015, **8**, 11–15.
- K. Szymańska, M. Pietrowska, J. Kocurek, K. Maresz, A. Koreniuk, J. Mrowiec-Białoń, P. Widłak, E. Magner and A. Jarzębski, *Chem. Eng. J.*, 2016, **287**, 148–154.
- C. Hoffmann, I. P. R. Grundtvig, J. Thrane, N. Garg, K. V. Gernaey, M. Pinelo, J. M. Woodley, U. Krühne and A. E. Daugaard, *Chem. Eng. J.*, 2018, **332**, 16–23.
- K. Nakagawa, A. Tamura and C. Chaiya, *Chem. Eng. Sci.*, 2014, **119**, 22–29.

- 47 D. B. Weibel, W. R. DiLuzio and G. M. Whitesides, *Nat. Rev. Microbiol.*, 2007, **5**, 209.
- 48 Y. Xia and G. M. Whitesides, *Angew. Chem., Int. Ed.*, 1998, **37**, 550–575.
- 49 D. Qin, Y. Xia and G. M. Whitesides, *Nat. Protoc.*, 2010, **5**, 491.
- 50 M. Focke, D. Kosse, C. Müller, H. Reinecke, R. Zengerle and F. von Stetten, *Lab Chip*, 2010, **10**, 1365–1386.
- 51 R. Truckenmüller, S. Giselbrecht, C. van Blitterswijk, N. Dambrowsky, E. Gottwald, T. Mappes, A. Rolletschek, V. Saile, C. Trautmann and K.-F. Weibezahn, *Lab Chip*, 2008, **8**, 1570–1579.
- 52 S.-J. J. Lee and N. Sundararajan, *Microfabrication for microfluidics*, Artech house, 2010.
- 53 C.-W. Tsao and D. L. DeVoe, *Microfluid. Nanofluid.*, 2009, **6**, 1–16.
- 54 C. Iliescu, H. Taylor, M. Avram, J. Miao and S. Franssila, *Biomicrofluidics*, 2012, **6**, 016505.
- 55 C.-W. Tsao, *Micromachines*, 2016, **7**, 225.
- 56 P. Kim, K. W. Kwon, M. C. Park, S. H. Lee, S. M. Kim and K. Y. Suh, *BioChip J.*, 2008, **2**, 1–11.
- 57 E. Peris, O. Okafor, E. Kulcinskaia, R. Goodridge, S. V. Luis, E. Garcia-Verdugo, E. O'Reilly and V. Sans, *Green Chem.*, 2017, **19**, 5345–5349.
- 58 S. Waheed, J. M. Cabot, N. P. Macdonald, T. Lewis, R. M. Guijt, B. Paull and M. C. Breadmore, *Lab Chip*, 2016, **16**, 1993–2013.
- 59 A. K. Au, W. Huynh, L. F. Horowitz and A. Folch, *Angew. Chem., Int. Ed.*, 2016, **55**, 3862–3881.
- 60 D. Pranzo, P. Larizza, D. Filippini and G. Percoco, *Micromachines*, 2018, **9**, 374.
- 61 J. S. Lee, S. H. Lee, J. H. Kim and C. B. Park, *Lab Chip*, 2011, **11**, 2309–2311.
- 62 A. Küchler, J. N. Bleich, B. Sebastian, P. S. Dittrich and P. Walde, *ACS Appl. Mater. Interfaces*, 2015, **7**, 25970–25980.
- 63 M. Jannat and K.-L. Yang, *Langmuir*, 2018, **34**, 14226–14233.
- 64 Y. Zhu, Z. Huang, Q. Chen, Q. Wu, X. Huang, P.-K. So, L. Shao, Z. Yao, Y. Jia, Z. Li, W. Yu, Y. Yang, A. Jian, S. Sang, W. Zhang and X. Zhang, *Nat. Commun.*, 2019, **10**, 4049.
- 65 Y. Lv, Z. Lin, T. Tan and F. Svec, *Biotechnol. Bioeng.*, 2014, **111**, 50–58.
- 66 F. Liu, Y. Piao, J. S. Choi and T. S. Seo, *Biosens. Bioelectron.*, 2013, **50**, 387–392.
- 67 A. Gong, C.-T. Zhu, Y. Xu, F.-Q. Wang, F.-A. Wu and J. Wang, *Sci. Rep.*, 2017, **7**, 4309.
- 68 N. Singh, M. A. Ali, P. Rai, A. Sharma, B. D. Malhotra and R. John, *ACS Appl. Mater. Interfaces*, 2017, **9**, 33576–33588.
- 69 Z. Yin, W. Zhao, M. Tian, Q. Zhang, L. Guo and L. Yang, *Analyst*, 2014, **139**, 1973–1979.
- 70 D. Valikhani, J. M. Bolivar, M. Viehwues, D. N. McIlroy, E. X. Vrouwe and B. Nidetzky, *ACS Appl. Mater. Interfaces*, 2017, **9**, 34641–34649.
- 71 J. Liu, X. Jiang, R. Zhang, Y. Zhang, L. Wu, W. Lu, J. Li, Y. Li and H. Zhang, *Adv. Funct. Mater.*, 2019, **29**, 1807326.
- 72 Y. Liu, W. Zhong, S. Meng, J. Kong, H. Lu, P. Yang, H. H. Girault and B. Liu, *Chem. – Eur. J.*, 2006, **12**, 6585–6591.
- 73 H. Bao, Q. Chen, L. Zhang and G. Chen, *Analyst*, 2011, **136**, 5190–5196.
- 74 Y. Bi, H. Zhou, H. Jia and P. Wei, *Process Biochem.*, 2017, **54**, 73–80.
- 75 G. H. Seong and R. M. Crooks, *J. Am. Chem. Soc.*, 2002, **124**, 13360–13361.
- 76 C. R. Boehm, P. S. Freemont and O. Ces, *Lab Chip*, 2013, **13**, 3426–3432.
- 77 S. Kundu, A. S. Bhangale, W. E. Wallace, K. M. Flynn, C. M. Guttman, R. A. Gross and K. L. Beers, *J. Am. Chem. Soc.*, 2011, **133**, 6006–6011.
- 78 J. Wang, X. Liu, X.-D. Wang, T. Dong, X.-Y. Zhao, D. Zhu, Y.-Y. Mei and G.-H. Wu, *Bioresour. Technol.*, 2016, **220**, 132–141.
- 79 G. H. Seong, J. Heo and R. M. Crooks, *Anal. Chem.*, 2003, **75**, 3161–3167.
- 80 L. C. Lasave, S. M. Borisov, J. Ehgartner and T. Mayr, *RSC Adv.*, 2015, **5**, 70808–70816.
- 81 D. N. Kim, Y. Lee and W.-G. Koh, *Sens. Actuators, B*, 2009, **137**, 305–312.
- 82 A. Kecskemeti and A. Gaspar, *Talanta*, 2017, **166**, 275–283.
- 83 T. Peschke, M. Skoupi, T. Burgahn, S. Gallus, I. Ahmed, K. S. Rabe and C. M. Niemeyer, *ACS Catal.*, 2017, **7**, 7866–7872.
- 84 R.-P. Liang, X.-N. Wang, C.-M. Liu, X.-Y. Meng and J.-D. Qiu, *J. Chromatogr. A*, 2013, **1315**, 28–35.
- 85 J. Sheng, L. Zhang, J. Lei and H. Ju, *Anal. Chim. Acta*, 2012, **709**, 41–46.
- 86 A. Karim, J. Bravo, D. Gorm, T. Conant and A. Datye, *Catal. Today*, 2005, **110**, 86–91.
- 87 J. M. Bolivar, J. Wiesbauer and B. Nidetzky, *Trends Biotechnol.*, 2011, **29**, 333–342.
- 88 D. J. Strub, K. Szymańska, Z. Hrydziszko, J. Bryjak and A. B. Jarzębski, *React. Chem. Eng.*, 2019, **4**, 587–594.
- 89 M. Petro, F. Svec and J. M. Fréchet, *Biotechnol. Bioeng.*, 1996, **49**, 355–363.
- 90 T. R. Besanger, R. J. Hodgson, J. R. Green and J. D. Brennan, *Anal. Chim. Acta*, 2006, **564**, 106–115.
- 91 J. Qiao, L. Qi, X. Mu and Y. Chen, *Analyst*, 2011, **136**, 2077–2083.
- 92 A. S. de León, N. Vargas-Alfredo, A. Gallardo, A. Fernández-Mayoralas, A. Bastida, A. Muñoz-Bonilla and J. Rodríguez-Hernández, *ACS Appl. Mater. Interfaces*, 2017, **9**, 4184–4191.
- 93 K. Nakagawa and Y. Goto, *Chem. Eng. Process.*, 2015, **91**, 35–42.
- 94 J. P. Lafleur, S. Senkbeil, J. Novotny, G. Nys, N. Bøgelund, K. D. Rand, F. Foret and J. P. Kutter, *Lab Chip*, 2015, **15**, 2162–2172.
- 95 T. C. Logan, D. S. Clark, T. B. Stachowiak, F. Svec and J. M. Fréchet, *Anal. Chem.*, 2007, **79**, 6592–6598.
- 96 D. S. Peterson, T. Rohr, F. Svec and J. M. Fréchet, *Anal. Chem.*, 2002, **74**, 4081–4088.
- 97 O. Yesil-Celiktas, S. Cumana and I. Smirnova, *Chem. Eng. J.*, 2013, **234**, 166–172.

- 98 M. Alotaibi, J. Manayil, G. M. Greenway, S. J. Haswell, S. M. Kelly, A. F. Lee, W. Karen and G. Kyriakou, *React. Chem. Eng.*, 2017, **3**, 68–74.
- 99 P. He, B. P. Burke, G. S. Clemente, N. Brown, N. Pamme and S. J. Archibald, *React. Chem. Eng.*, 2016, **1**, 361–365.
- 100 Y. Yi, Y. Chen, M. A. Brook and J. D. Brennan, *Chem. Mater.*, 2006, **18**, 5336–5342.
- 101 J. Ma, Z. Liang, X. Qiao, Q. Deng, D. Tao, L. Zhang and Y. Zhang, *Anal. Chem.*, 2008, **80**, 2949–2956.
- 102 P. Liang, H. Bao, J. Yang, L. Zhang and G. Chen, *Carbon*, 2016, **97**, 25–34.
- 103 D. Pirozzi, M. Abagnale, L. Minieri, P. Pernice and A. Aronne, *Chem. Eng. J.*, 2016, **306**, 1010–1016.
- 104 D. N. Tran and K. J. Balkus Jr, *ACS Catal.*, 2011, **1**, 956–968.
- 105 J. Ma, L. Zhang, Z. Liang, W. Zhang and Y. Zhang, *J. Sep. Sci.*, 2007, **30**, 3050–3059.
- 106 J. Nelson and E. G. Griffin, *J. Am. Chem. Soc.*, 1916, **38**, 1109–1115.
- 107 T. Honda, H. Yamaguchi and M. Miyazaki, *Applied Bioengineering: Innovations and Future Directions*, 2017, vol. 5.
- 108 L. Cao, in *Carrier-bound Immobilized Enzymes*, Wiley-VCH Verlag GmbH & Co. KGaA, 2006, DOI: 10.1002/3527607668. ch2, pp. 53–168.
- 109 M. L. Shuler, F. Kargi and F. Kargi, *Bioprocess engineering: basic concepts*, Prentice Hall, Upper Saddle River, NJ, 2002.
- 110 Z.-m. Tang and J.-w. Kang, *Anal. Chem.*, 2006, **78**, 2514–2520.
- 111 A. Srinivasan, H. Bach, D. H. Sherman and J. S. Dordick, *Biotechnol. Bioeng.*, 2004, **88**, 528–535.
- 112 G. Kulsharova, N. Dimov, M. P. Marques, N. Szita and F. Baganz, *New Biotechnol.*, 2017, **47**, 31–38.
- 113 H. Mao, T. Yang and P. S. Cremer, *Anal. Chem.*, 2002, **74**, 379–385.
- 114 M. A. Holden, S.-Y. Jung and P. S. Cremer, *Anal. Chem.*, 2004, **76**, 1838–1843.
- 115 T. Vong, S. Schoffelen, S. F. van Dongen, T. A. van Beek, H. Zuilhof and J. C. van Hest, *Chem. Sci.*, 2011, **2**, 1278–1285.
- 116 Z.-Q. Wu, Z.-Q. Li, J.-Y. Li, J. Gu and X.-H. Xia, *Phys. Chem. Chem. Phys.*, 2016, **18**, 14460–14465.
- 117 K. Sakai-Kato, M. Kato and T. Toyo'oka, *Anal. Chem.*, 2003, **75**, 388–393.
- 118 H. Wu, Y. Tian, B. Liu, H. Lu, X. Wang, J. Zhai, H. Jin, P. Yang, Y. Xu and H. Wang, *J. Proteome Res.*, 2004, **3**, 1201–1209.
- 119 S.-i. Matsuura, R. Ishii, T. Itoh, S. Hamakawa, T. Tsunoda, T. Hanaoka and F. Mizukami, *Chem. Eng. J.*, 2011, **167**, 744–749.
- 120 W.-G. Koh and M. Pishko, *Sens. Actuators, B*, 2005, **106**, 335–342.
- 121 A. A. Homaei, R. Sariri, F. Vianello and R. Stevanato, *J. Chem. Biol.*, 2013, **6**, 185–205.
- 122 X. Ji, F. Ye, P. Lin and S. Zhao, *Talanta*, 2010, **82**, 1170–1174.
- 123 W. Min, W. Wang, J. Chen, A. Wang and Z. Hu, *Anal. Bioanal. Chem.*, 2012, **404**, 2397–2405.
- 124 J. J. Virgen-Ortíz, J. C. dos Santos, Á. Berenguer-Murcia, O. Barbosa, R. C. Rodrigues and R. Fernandez-Lafuente, *J. Mater. Chem. B*, 2017, **5**, 7461–7490.
- 125 S. Zhao, X. Ji, P. Lin and Y.-M. Liu, *Anal. Biochem.*, 2011, **411**, 88–93.
- 126 T.-F. Jiang, T.-T. Liang, Y.-H. Wang, W.-H. Zhang and Z.-H. Lv, *J. Pharm. Biomed. Anal.*, 2013, **84**, 36–40.
- 127 M. A. Camara, M. Tian, L. Guo and L. Yang, *J. Chromatogr., B*, 2015, **990**, 174–180.
- 128 Z. Tang, T. Wang and J. Kang, *Electrophoresis*, 2007, **28**, 2981–2987.
- 129 F. Wang, C. Guo, H.-Z. Liu and C.-Z. Liu, *J. Mol. Catal. B: Enzym.*, 2007, **48**, 1–7.
- 130 D. Kirstein, *Adv. Mol. Cell Biol.*, 1996, **15**, 247–256.
- 131 Q.-H. Shi, Y. Tian, X.-Y. Dong, S. Bai and Y. Sun, *Biochem. Eng. J.*, 2003, **16**, 317–322.
- 132 M. Miyazaki, J. Kaneno, R. Kohama, M. Uehara, K. Kanno, M. Fujii, H. Shimizu and H. Maeda, *Chem. Eng. J.*, 2004, **101**, 277–284.
- 133 B. Brena, P. González-Pombo and F. Batista-Viera, *Immobilization of Enzymes and Cells: Third Edition*, 2013, pp. 15–31.
- 134 P. C. Weber, D. Ohlendorf, J. Wendoloski and F. Salemme, *Science*, 1989, **243**, 85–88.
- 135 F. Rusmini, Z. Zhong and J. Feijen, *Biomacromolecules*, 2007, **8**, 1775–1789.
- 136 A. González-Campo, B. Eker, H. J. Gardeniers, J. Huskens and P. Jonkheijm, *Small*, 2012, **8**, 3531–3537.
- 137 H. Schröder, L. Hoffmann, J. Müller, P. Alhorn, M. Fleger, A. Neyer and C. M. Niemeyer, *Small*, 2009, **5**, 1547–1552.
- 138 D. Liu, R. K. Perdue, L. Sun and R. M. Crooks, *Langmuir*, 2004, **20**, 5905–5910.
- 139 L. Lloret, G. Eibes, M. Moreira, G. Feijoo, J. Lema and M. Miyazaki, *Chem. Eng. J.*, 2013, **223**, 497–506.
- 140 C. D. Blanchette, J. M. Knipe, J. K. Stolaroff, J. R. DeOtte, J. S. Oakdale, A. Maiti, J. M. Lenhardt, S. Sirajuddin, A. C. Rosenzweig and S. E. Baker, *Nat. Commun.*, 2016, **7**, 11900.
- 141 D. Simon, F. Obst, S. Haefner, T. Heroldt, M. Peiter, F. Simon, A. Richter, B. Voit and D. Appelhans, *React. Chem. Eng.*, 2019, **4**, 67–77.
- 142 S. Cumana, J. Simons, A. Liese, L. Hilterhaus and I. Smirnova, *J. Mol. Catal. B: Enzym.*, 2013, **85**, 220–228.
- 143 G. Ranieri, R. Mazzei, Z. Wu, K. Li and L. Giorno, *Molecules*, 2016, **21**, 345.
- 144 M. Bajić, I. Plazl, R. Stloukal and P. Žnidaršič-Plazl, *Process Biochem.*, 2017, **52**, 63–72.
- 145 H. Tan, S. Guo, N.-D. Dinh, R. Luo, L. Jin and C.-H. Chen, *Nat. Commun.*, 2017, **8**, 663.
- 146 H. Wang, Z. Zhao, Y. Liu, C. Shao, F. Bian and Y. Zhao, *Sci. Adv.*, 2018, **4**, eaat2816.
- 147 S. Fornera, P. Kuhn, D. Lombardi, A. D. Schlüter, P. S. Dittrich and P. Walde, *ChemPlusChem*, 2012, **77**, 98–101.
- 148 F. Costantini, R. Tiggelaar, S. Sennato, F. Mura, S. Schlaутmann, F. Bordi, H. Gardeniers and C. Manetti, *Analyst*, 2013, **138**, 5019–5024.

- 149 T. Peschke, P. Bitterwolf, S. Gallus, Y. Hu, C. Oelschlaeger, N. Willenbacher, K. S. Rabe and C. M. Niemeyer, *Angew. Chem.*, 2018, **130**, 17274–17278.
- 150 R. J. Conrado, J. D. Varner and M. P. DeLisa, *Curr. Opin. Biotechnol.*, 2008, **19**, 492–499.
- 151 Y.-H. P. Zhang, *Biotechnol. Adv.*, 2011, **29**, 715–725.
- 152 A. Küchler, M. Yoshimoto, S. Luginbühl, F. Mavelli and P. Walde, *Nat. Nanotechnol.*, 2016, **11**, 409–420.
- 153 T. Vong, S. Schoffelen, S. F. M. van Dongen, T. A. van Beek, H. Zuilhof and J. C. M. van Hest, *Chem. Sci.*, 2011, **2**, 1278–1285.
- 154 J. Grant, J. A. Modica, J. Roll, P. Perkovich and M. Mrksich, *Small*, 2018, **14**, 1800923.
- 155 G. Palazzo, G. Colafemmina, C. G. Iudice and A. Mallardi, *Sens. Actuators, B*, 2014, **202**, 217–223.
- 156 J. Heo, *Anal. Sci.*, 2014, **30**, 991–997.
- 157 S. Schoffelen and J. C. van Hest, *Curr. Opin. Struct. Biol.*, 2013, **23**, 613–621.
- 158 J. Fu, M. Liu, Y. Liu, N. W. Woodbury and H. Yan, *J. Am. Chem. Soc.*, 2012, **134**, 5516–5519.
- 159 V. Hessel, C. Knobloch and H. Lowe, *Recent Pat. Chem. Eng.*, 2008, **1**, 1–16.
- 160 N. Kockmann, M. Gottsponer, B. Zimmermann and D. M. Roberge, *Chem. – Eur. J.*, 2008, **14**, 7470–7477.
- 161 N. Kockmann, M. Gottsponer and D. M. Roberge, *Chem. Eng. J.*, 2011, **167**, 718–726.
- 162 N. Kockmann and D. M. Roberge, *Chem. Eng. Process.*, 2011, **50**, 1017–1026.
- 163 P. Žnidaršič-Plazl, *Biotechnol. J.*, 2019, **14**, 1800580.
- 164 N. Miložić, M. Lubej, M. Lakner, P. Žnidaršič-Plazl and I. Plazl, *Chem. Eng. J.*, 2017, **313**, 374–381.
- 165 F. Strniša, M. Bajić, P. Panjan, I. Plazl, A. M. Sesay and P. Žnidaršič-Plazl, *Chem. Eng. J.*, 2018, **350**, 541–550.
- 166 A. Šalić, P. Faletar and B. Zelić, *Biochem. Eng. J.*, 2013, **77**, 88–96.
- 167 J.-i. Yoshida, *Flash chemistry: Fast organic synthesis in microsystems*, John Wiley & Sons, 2008.
- 168 S. J. Haswell and P. Watts, *Green Chem.*, 2003, **5**, 240–249.
- 169 S. G. Newman and K. F. Jensen, *Green Chem.*, 2013, **15**, 1456–1472.
- 170 C. Amador, A. Gavriliidis and P. Angeli, *Chem. Eng. J.*, 2004, **101**, 379–390.
- 171 Z. Liu, J. Zhang, X. Chen and P. G. Wang, *ChemBioChem*, 2002, **3**, 348–355.
- 172 B. Orsat, B. Wirz and S. Bischof, *Chimia*, 1999, **53**, 579–584.
- 173 G. Gasparini, I. Archer, E. Jones and R. Ashe, *Org. Process Res. Dev.*, 2012, **16**, 1013–1016.
- 174 U. Novak, D. Lavric and P. Žnidaršič-Plazl, *J. Flow Chem.*, 2016, **6**, 33–38.
- 175 S. Pithani, S. Karlsson, H. Emténäs and C. T. Öberg, *Org. Process Res. Dev.*, 2019, **23**, 1926–1931.
- 176 R. Das, H. Mishra, A. Srivastava and A. M. Kayastha, *Chem. Eng. J.*, 2017, **328**, 215–227.
- 177 H.-L. Shuai, K.-J. Huang, Y.-X. Chen, L.-X. Fang and M.-P. Jia, *Biosens. Bioelectron.*, 2017, **89**, 989–997.
- 178 J. Sun, R. Yendluri, K. Liu, Y. Guo, Y. Lvov and X. Yan, *Phys. Chem. Chem. Phys.*, 2017, **19**, 562–567.
- 179 A. A. Kadam, J. Jang and D. S. Lee, *ACS Appl. Mater. Interfaces*, 2017, **9**, 15492–15501.
- 180 M. Z. Anwar, D. J. Kim, A. Kumar, S. K. Patel, S. Otari, P. Mardina, J.-H. Jeong, J.-H. Sohn, J. H. Kim and J. T. Park, *Sci. Rep.*, 2017, **7**, 15333.
- 181 X. Lian, Y. Fang, E. Joseph, Q. Wang, J. Li, S. Banerjee, C. Lollar, X. Wang and H.-C. Zhou, *Chem. Soc. Rev.*, 2017, **46**, 3386–3401.
- 182 P. Li, J. A. Modica, A. J. Howarth, E. Vargas, P. Z. Moghadam, R. Q. Snurr, M. Mrksich, J. T. Hupp and O. K. Farha, *Chem.*, 2016, **1**, 154–169.
- 183 Z. Li, H. Xia, S. Li, J. Pang, W. Zhu and Y. Jiang, *Nanoscale*, 2017, **9**, 15298–15302.